Isolated DC-DC Converter with High-Frequency Transformer for EV Charging

A PROJECT REPORT

SUBMITTED IN PARTIAL FULFILLMENT OF THE REQUIREMENTS
FOR THE AWARD OF THE DEGREE
OF

MASTER OF TECHNOLOGY

IN

POWER ELECTRONICS AND SYSTEMS

Submitted by

Awanish Akash

(2K21/PES/06)

Under the supervision of

Prof. Mini Sreejeth

DEPARTMENT OF ELECTRICAL ENGINEERING

DELHI TECHNOLOGICAL UNIVERSITY

(Formerly Delhi College of Engineering) Bawana Road, Delhi-110042

May 2023

DEPARTMENT OF ELECTRICAL ENGINEERING
DELHI TECHNOLOGICAL UNIVERSITY
(Formerly Delhi College of Engineering)
Bawana Road, Delhi-110042

CANDIDATE'S DECLARATION

I, Awanish Akash, Roll No –2K21/PES/06 student of M. Tech (Power Electronics & System), hereby declare that the project Dissertation titled "Isolated DC-DC converter with High-Frequency Transformer for EV Charging" which is submitted by me to the Electrical Engineering, Delhi Technological University, Delhi in partial fulfillment of the requirement for the award of the degree of Master of Technology is original and not copied from any source without proper citation. This work has not previously formed the basis for the award of any Degree, Diploma Associateship, Fellowship, or other similar title or recognition.

Place: Delhi Awanish Akash(2K21/PES/06)

Date: 31.05.2023

DEPARTMENT OF ELECTRICAL ENGINEERING
DELHI TECHNOLOGICAL UNIVERSITY
(Formerly Delhi College of Engineering)
Bawana Road, Delhi-110042

CERTIFICATE

I certify that the Project Dissertation titled "Isolated DC-DC Converter with High-Frequency Transformer for EV Charging" was submitted by Awanish Akash, Roll No – 2K21/PES/06. here, Electrical Engineering, Delhi Technological University, Delhi in partial fulfilment of the requirement for the award of the degree of Master of Technology, is a record of the project work carried out by the students under my supervision. To the best of my knowledge, this work has not been submitted in part or full for any Degree or Diploma to this University or elsewhere.

SUPERVISOR
Prof. Mini Sreejeth

Place: Delhi

Date: 31.05.2023

ABSTRACT

The use of Electric Vehicles (EVs) is increasing day by day and therefore chargers for electric vehicles play a vital role in the evolution of the industry. The EVs have zero emissions which are good for the atmosphere. The extensive dependency on Fossil fuels has to be taken care of by switching to eco-friendly EVs. In terms of efficiency, 60 % of the total electrical energy available from the grid is converted to useful work of powering the wheel whereas, in the case of traditional IC engine vehicles, only 17% to 20% of total energy available from the fuel is used in powering the wheel which shows that there is 80% wastage of the fuel energy. Even if the production of electricity is considered for EVs then IC engines have 3 times more carbon monoxide emissions than the average EVs. EVs have lower running costs and maintenance. DC-DC converter is an important part of EV chargers.

The study presents the PSFB (phase-shifted full bridge) dc-dc converter with diode rectification and synchronous rectification. To obtain higher levels of efficiency, PSFB with synchronous rectification is preferred. The converter supports zero voltage switching (ZVS) which aids the converter to work at high frequencies along with advantages like less EMI (Electromagnetic Interference), less stress, lower switching losses, and better efficiency. The PSFB converter with the input DC voltage at 380 V under the zero voltage conditions for both the cases Rectification and Synchronous Rectification at different loads have been studied. The topology utilizes the resonance between the leakage inductor of the high-frequency transformer and parasitic capacitances of full bridge MOSFETS for achieving ZVS. If the current or voltage is zero during the transient in the MOSFET switch, the soft switching is visible. Zero current switching (ZCS) and zero voltage switching are two soft switching techniques (ZVS). Here in the paper, ZVS has been implemented resulting in minimum switching losses.

The study also proposes a closed-loop control approach for a PSFB (phase-shifted full bridge) dc-dc converter operating under synchronous rectification for EV charging applications. A 48V Lithium Ion Battery has been used for the charging process and one PI controller has been implemented for CC (Constant Current) mode charging. The system is designed for the listed specifications, and the analysis is carried out using MATLAB/Simulink software.

DEPARTMENT OF ELECTRICAL ENGINEERING
DELHI TECHNOLOGICAL UNIVERSITY
(Formerly Delhi College of Engineering)
Bawana Road, Delhi-110042

ACKNOWLEDGEMENT

I wish to express my sincerest gratitude to Prof. Mini Sreejeth for the continuous guidance and mentorship that she provided me during the project. She showed me the path to achieve the targets by explaining all the tasks to be done and explaining to me the importance of this project as well as its industrial relevance. She was always ready to help me and clear my doubts regarding any hurdles in this project. Without her constant support and motivation, this project would not have been successful. Finally, I would like to recognize the Department of EE for accepting me into the program and allowing me to pursue my interests in Power electronics & Systems.

Place: Delhi Awanish Akash(2K21/PES/06)

Date: 31.05.2023

CONTENTS

LIST OF FIGURES

LIST OF TABLES

LIST OF SYMBOLS, ABBREVIATIONS

Symbols

Ω	ohm
%	Percentage
V	Volt
A	Ampere
L	Inductance
Fs	Switching frequency
Vin	Input Voltage
Vo	Output Voltage
Lm	Magnetizing inductance
Co	Output Capacitance
D	Duty cycle
T	Time Period
Vp	The voltage at primary side
Vs	The voltage at secondary side
C_{mos}	Capacitance across switch
Kp	Proportional constant
Ki	Integral constant
Kd	Derivative constant
Vref	Reference voltage
C_{tr}	Transformer winding capacitance

Abbreviations

EV	Electric Vehicle
MOSFET	Metal oxide semiconductor field effect transistor
ZVS	Zero Voltage Switching
IGBT	Insulated Gate Bipolar Transistor
V2G	Vehicle to Grid
CC	Constant Current
CV	Constant voltage
SOC	State of charge
CC-CV	Constant voltage- Constant current
DC	Direct Current
PID	Proportional Integral Derivative

CHAPTER 1
INTRODUCTION

As the human population is growing dramatically in the modern era, car demand is increasing. Rising vehicle demand and heavy reliance on oil for transportation compel the extraction of more and more fossil fuels like diesel and petrol. Today, the primary challenges are the limited availability of fossil fuels and the pollution produced by them. Stocks are limited and demand is increasing, whereby due to the increased consumption, pollution is contributing majorly to degrading the environment and its entities. Consequently, to address these issues Electric vehicles (EVs) are essential to modern architecture and are urgently needed. The primary benefits of EV adoption mostly involve reducing transportation's dependency on oil and reducing carbon emissions. In case there's doesn't exist other transportation options, a lack of oil could cause sharp price increases in the oil business.

1.1 BACKGROUND OF THE PROJECT

Robert Davidson invented the first electric locomotive concept in 1837, and the first electric locomotive was used on a main line in 1895 on the 4-mile-long Baltimore Beltline in the United States. At the beginning of the 19th century, electric vehicles (EVs) began to expand, and the first experiments were conducted on electric trams and tram cars. By the end of the 19th century, however, EVs came into being used widely due to the mass production of rechargeable batteries, which had brought about a revolutionary change in the EV industry and had emerged as a key player. In 1881, the first-ever regular tram service was inaugurated in the German city of Berlin. Halske and Siemens worked together on this project. As time went on and we entered the 20th century, private automobiles were still uncommon but electric in nature. Although the EV sector was expanding, issues with batteries were also a concern because they required more time to recharge and cost more than equivalent-sized IC engines, which meant that during the entire 20th century, IC engines predominated. After then, the idea of a hybrid car with an internal combustion engine and one or more electric units was introduced. Ferdinand Porsche first unveiled a hybrid car that could run on power generated by either the engine or the batteries in 1900. Due to their minimal maintenance needs, electric trains became popular with railroads in the middle of the 20th century. Electric trains have been very successful because of overhead power lines, but electric cars haven't been as successful because they somehow rely on batteries. Still, EVs have some advantages over internal combustion engines

because they don't emit any exhaust emissions and are naturally quiet, which makes them ideal for industries where pollution and noise are a concern.

Coming at a time when high-speed train development was underway, during the end of the 20th and the beginning of the 21st centuries. The idea of a bullet train, whose services between Tokyo and Osaka began in 1964, was the catalyst for everything as it took 4 hours to travel 515.4 km of the trip. More advancements include Maglev trains, which travel on a specially designed track and have a top speed of 581 kph. They are in a race with aircraft to observe who can travel furthest more quickly. EV battery use and charging are the main problems, considering that several manufacturers are already making high-quality EVs. Renault, Mitsubishi, Nissan, and Tesla are a few of them. Following 1990, electric bicycles became popular and electric two-wheelers also gained growth. Hybrid vehicles, along with solar power and AC charging, are another new area of research that has to be further investigated. Promoting EVs is helping to reduce dangerous greenhouse gases and is suited while taking into account environmental concerns for the high-efficiency needs in the automotive industry[1],[2]. Additionally, a variety of motor control techniques are accessible, which improves the use of EVs in the automotive sector. The points presented above support the need for EV in the modern world. Electric rickshaws, electric bicycles, electric trains, and electric cars are a few instances of EVs in general. The Indian government aims 30% electric vehicle incorporation by 2030. To achieve this goal, it has been suggested that all two-wheelers with engines under 150cc should be electrified by March 2025 and all three-wheelers sold after March 31, 2025, should be electrified.

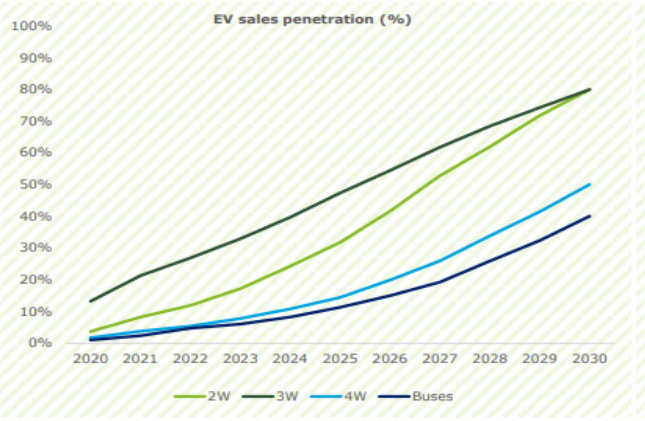

Fig.1.1 Sales as projected by NITI AAYOG

Figure 1.1 shows the EV sales as projected by NITI AAYOG by 2030. This would result in a saving of 474 MTE of oil annually and would cut down the emission of carbon dioxide by 846.3Mn tons annually.

1.2 Charging Configuration

Figure 1.2 shows the general charging configuration. It involves two stages of conversion ac to dc and then dc to dc, later on, the power is fed to the battery. In the study report, the prime focus is on the topology of the DC-DC converter which results in efficient charging [3].

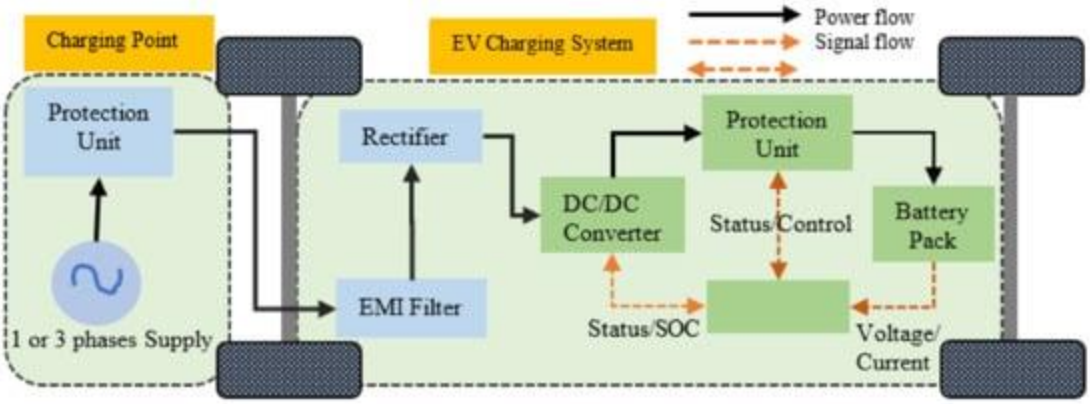

Fig.1.2. EV Charging System

1.3 Charging Power Levels

Charger power levels are a reflection of power, charging location and time, price, equipment, and grid impact. The deployment of the electric vehicle supply equipment (EVSE) and charging stations is a crucial first step since there are numerous concerns that must be resolved, including demand, scope, distribution, policies designed to fulfill those demands, standardization of charging stations, and regulatory procedures[4],[5]. Customers prefer to charge their electric vehicles (EVs) at their own convenience most of the time, thus it will be quite convenient for them if the charging can happen overnight at home in a garage where you can plug the EV into a handy outlet. The levels of charging are basically classified into three levels:

Table 1.1: Classification of Power Level at the charging station

Charging Station Type	Power Supply	Charging Time
Level 1(AC)	120/230 V_{ac},12 A to 16 A (Single Phase)	16 to 20 hrs
Level 2(AC)	208/240 V_{ac}, 15 A to 80 A (Single/ Split Phase)	2 to 6 hrs

Level 3 (DC Fast)	300 – 600 V_{dc}, (Maximum current 400 A, Three phases)	Less than 1 hr
Upcoming Generation (Ultra-Fast)	800 V_{dc} and higher, 400 A and higher (Polyphase)	Less than 20 minutes

Level 1: It is a simple and slow charging system. In the US, it uses a typical grounded 120V/ 15A single-phase outlet. In an eight-hour overnight charge, it can increase the range by around 40 miles. Low- and medium-range plug-in hybrids as well as all-electric battery electric car users who don't drive very far each day can also benefit from overnight Level 1 charging.

Level 2: Level 2 charging is most frequently used at public charging stations. The level 2 equipment that is currently in use supports charging from 208V or 240V [6]. For residential or commercial premises, it might be necessary to construct a connection, even if some vehicles, like the Tesla, already have the power electronics on board and merely require an outlet. A common EV battery can be charged overnight using Level 2 devices [7],[8]. The new standard is designed to enable either ac or dc rapid charging via a single connection and has an SAE J1772 ac charge connector on top and a two-pin dc connector below.

Level 3: It offers the possibility of charging in less than 1 hour. Similar to petrol stations, it can be implemented in city refilling points and highway rest places. It commonly uses a three-phase circuit with a voltage of 480 V or greater and requires controlled ac-dc conversion, which is provided by an off-board charger. Direct DC connections can be made to the vehicle.

An advantage for utilities looking to reduce the on-peak impact is a lower charge power. High-power rapid charging has the ability to quickly overload local distribution equipment during peak hours and can increase demand. Levels 2 and 3 charging may result in an increase in peak demand, harmonic distortion, distribution system thermal loads, distribution transformer losses, and voltage deviations. The shorter transformer life could have a substantial influence on the reliability, security effectiveness, and economy of developing smart grids. The development of Level 3 DC Fast chargers has been prompted by their low power rating and long charging time. The different types of levels of charging depend on the type of power requirement [9],[10]. A proposed option that could charge an electric vehicle (EV) in a very short period of time is DC ultra-fast charging

1.4 ONBOARD CHARGER AND OFF-BOARD CHARGER

The placement and size of the charger, if present inside the car, influence its performance in a manner similar to how the location, size, and energy density of the battery affect the performance of the vehicle. The chargers can be divided primarily into two categories based on the location at which they are present:

1.) On Board Charger

2.) Off Board Charger

Due to the high power flow, chargers are preferred to be placed external to the vehicle thereby reducing the weight and the volume of the vehicle. In the case of Onboard chargers, it is located inside the vehicle whereas, in the case of Off-board chargers, it is directly connected to the vehicle[11],[12].

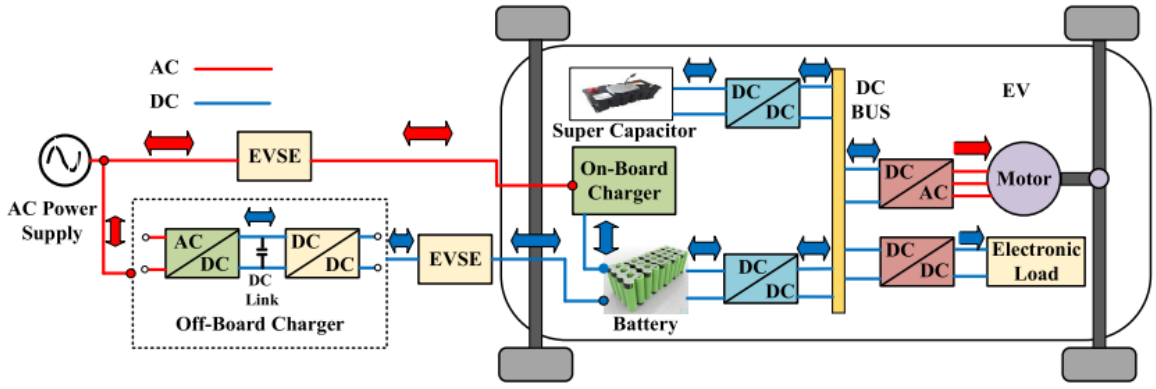

Fig.1.3 EV charging system showing off-board and onboard charger

Table 1.2: Comparison between Onboard charger and Offboard Charger [12]

Factors	Onboard Charger	Offboard Charger
Location	Inside the vehicle	Outside the Vehicle
Level	Limits the power to level 1	Allows level 2 and level 3
BMS	Low sophisticated BMS	A high sophisticated BMS is required
Space constraint	Less space constraint	More space constraint
Energy Transfer rate	Low	High

1.5 UNIDIRECTIONAL AND BIDIRECTIONAL CHARGERS

This classification has been done based on the direction of the power flow. The converter mechanism in EVs allows energy to move from the grid to the battery. The kind of switches used in the converter system determines the rush of energy. Switches ranging

from basic diodes to BJT, Thyristors, MOSFETs, IGBTs, DIACs, and TRIACs can be employed. BJTs, thyristors, and diodes are all unidirectional devices, allowing current to flow only in the positive direction. Being bidirectional devices, MOSFET and IGBTs allow current to flow in either way. Similar to this, electric vehicles are likewise divided into groups according to the system's energy flow:

1.) Unidirectional Charger
2.) Bidirectional Charger

Unidirectional Charger: The EV battery can be charged using unidirectional chargers, but energy cannot be returned to the electrical grid. As previously stated, it employs switches that only allow current to flow in one way, forward. As a result, it is capable of using unidirectional switches such as thyristors, BJTs, and diodes. It is preferred to use these converters in a single stage so that volume, weight, power density, cost, and losses can be kept to a minimum. Comparatively speaking, the unidirectional system's controlling topology is simpler than that of the bidirectional charging. Because of its simplicity, it is simpler to deploy and can control feeders that are heavily loaded and connected to a number of electric vehicles charging simultaneously.

Bidirectional Charger: It supports power flow in both directions that is grid to vehicle and vehicle to grid. At peak hours if the charge is left in the battery, then it can be used for the purpose of driving home appliances. Also, the customer can feed back the power into the grid thereby providing incentives to the customer.

A bidirectional switch is also called a four-quadrant switch. It allows two-way bidirectional flow of current when turned ON as shown in Figure 1.4 and also blocks the voltage of reverse polarities when turned OFF as shown in Figure 1.5

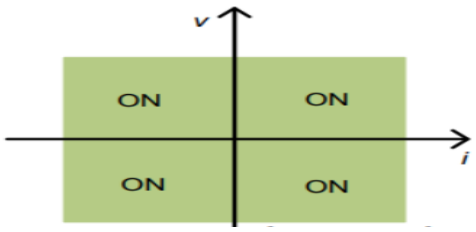

Fig. 1.4 Characteristics in ON state for the bidirectional switch

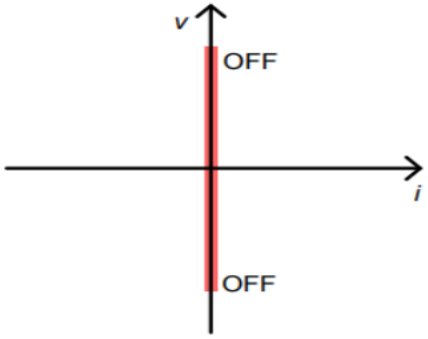

Fig.1.5. Characteristics in OFF state for the bidirectional switch

A Bidirectional Switch should be highly adaptable to power flow in both directions for quick and easy implementation. For use in DC regulation, the resistance between the source and drain should be kept low for better voltage regulation. A bidirectional switch should have protection circuitry features to withstand the sudden inrush of reverse current during the polarity change or at relatively higher temperature conditions. A Bidirectional switch is formed by connecting two MOSFETS back to back.[13]

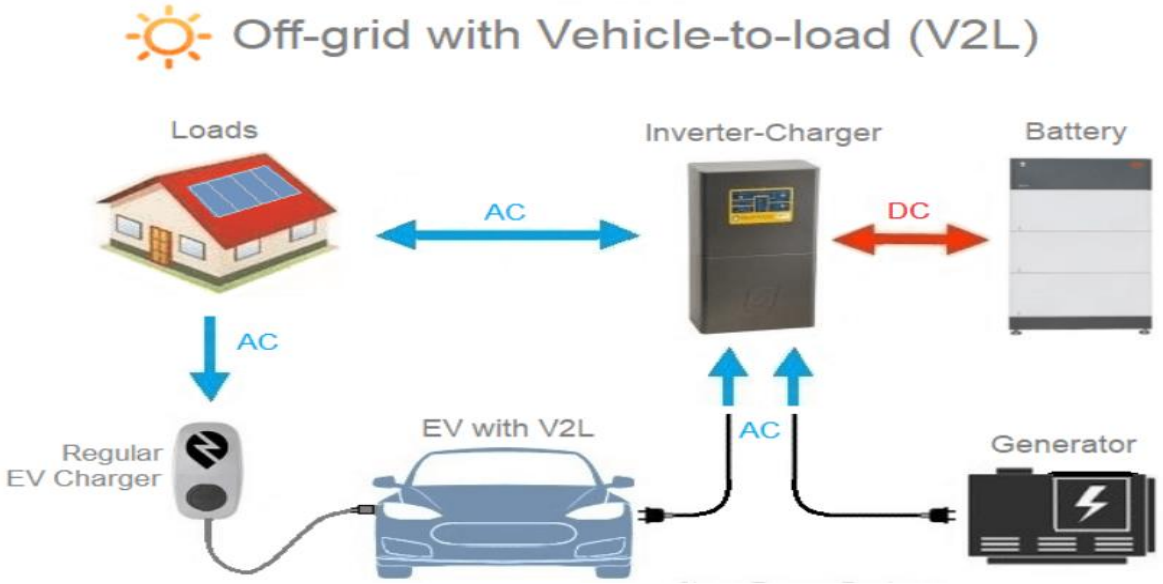

Fig 1.6 EV with Bidirectional Charger

Figure 1.6 shows the Electric Vehicle application in a bidirectional mode where the EV is getting charged from the Regular EV charger through an AC supply whereas the Battery of the EV can be seen providing power back to the loads. The bidirectional Mode of charging helps EVs get charged during off-peak hours and also supplies power to the grid during peak hours when there is high energy demand.

1.6 BATTERY IN ELECTRIC VEHICLES

One of the crucial elements that affect how well an EV performs is its battery. It is made up of electrochemical cells, and the vehicle is powered via connections to the outside world. From there, the technology for EV batteries began to develop [14],[15]. The development of the Technology for battery in EVs started in the late nineteenth century with lead acid batteries and later came across lithium-ion battery which is found in most EVs today. A battery pack consists of multiple battery modules and battery cells. Electric vehicle battery packs can contain as few as 96 battery cells or as many as 2,976 batteries. Primary and secondary are the two types. Vehicle batteries in this instance are often rechargeable backup batteries. The traction batteries are used by electric forklifts, golf carts, cars, lorries, vans, and other vehicles. SLI batteries, which stand for starting, ignition, and lighting, are one of the battery types. Lead-acid batteries of the SLI type, which are typically used in cars, are rechargeable. Deep cycle batteries are a different variety in which the battery is discharged much more thoroughly than other types. Vehicles with electricity-charged batteries are different from those with starting, lighting, and ignition (SLI) systems since they are made to provide power for extended periods of time. SLI batteries, which stand for starting, ignition, and lighting, are one of the battery types. Lead-acid batteries of the SLI type, which are typically used in cars, are rechargeable. Deep cycle batteries are a different variety in which the battery is discharged much more thoroughly than other types. Vehicles with electricity-charged batteries are different from those with starting, lighting, and ignition (SLI) systems since they are made to provide power for extended periods of time. Instead of SLI batteries, Deep cycle batteries are used for various application purposes. For designing traction batteries, it is done with a high ampere-hour capacity perspective. The battery for electric vehicles is characterized by

- The power-to-weight ratio should be high
- The energy density should be specific
- Smaller size

If the batteries are lighter then it provides the advantage that the weight of the vehicle reduces and performance is improved. The majority of existing battery technologies have substantially lower specific energies than liquid fuels, which affects the maximum all-electric range of the vehicles. Despite this, the metal-air batteries have a high specific energy because the oxygen in the air surrounds the cathode they use. A few examples include zinc-air, lithium-ion, lead-acid, lithium-ion polymer, nickel-metal hydride, and nickel-cadmium which are used in electric car rechargeable batteries [16],[17]. Due to their

high energy density in relation to their weight, lithium-ion, and lithium-polymer batteries are the most popular battery types in contemporary electric vehicles. The amount of electrical energy stored in the batteries is expressed in Ampere-hours.

The following are some of the advantages of Lithium-ion batteries:

1.) One of the best features is high power density. When it comes to offering the same level of capacity, Li-ion batteries are lighter than other battery kinds.

2.) Compared to lead-acid (4–6%) and nickel-metal hydride (30%) batteries, lithium-ion cells self-discharge at a rate of 2–3 percent each month. As a result, the Li-ion battery has a significantly longer expected lifespan than other battery types. The discharge curve of the lithium-ion battery is also flat. For high-energy applications, it is well known that if the battery's power output reduces quickly during the discharging period, a dangerous problem may develop towards the end of the period. For around 80% of the discharge cycle, the lithium-ion battery provides voltages that are practically constant [18],[19].

3.) A lithium-ion battery pack has a large number of cells within. For instance, the 196 cells in the Nissan Leaf battery packs are composed of 48 modules, each of which has four cells. With this setup, charging happens faster and more effectively.

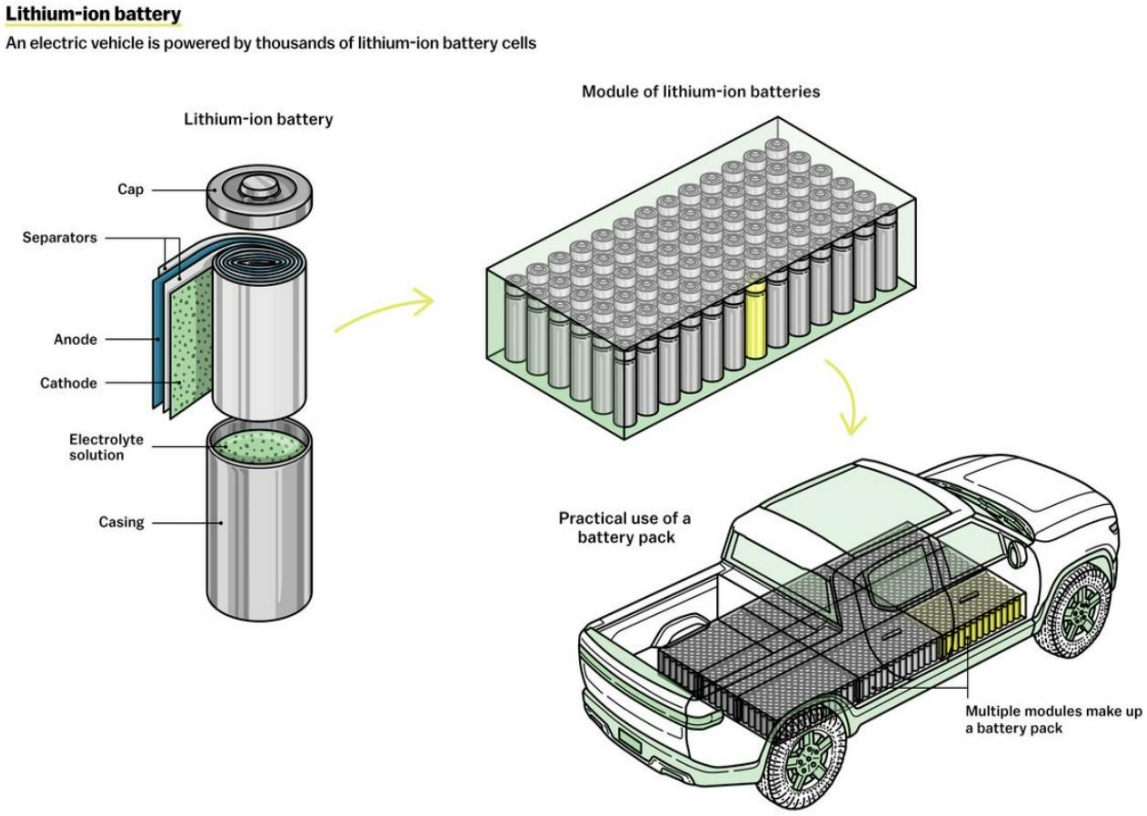

Fig.1.7 Lithium-ion Battery in Electric Vehicle

Figure 1.7 shows the lithium-ion battery and its packaging in EVs. An electric vehicle is powered by thousands of lithium-ion battery cells. It can be seen in the figure Lithium-ion Battery consists of Cap, Separators, Anode, Cathode, Electrolyte solution and Casing.

Table 1.3: Comparison between three primary types of battery used in EV

TYPE	COST	LIFE	ENERGY DENSITY
LEAD-ACID	Affordable	Low	Good
Ni-MH	High	High	Good
Li-ion	Reasonable	High	Good

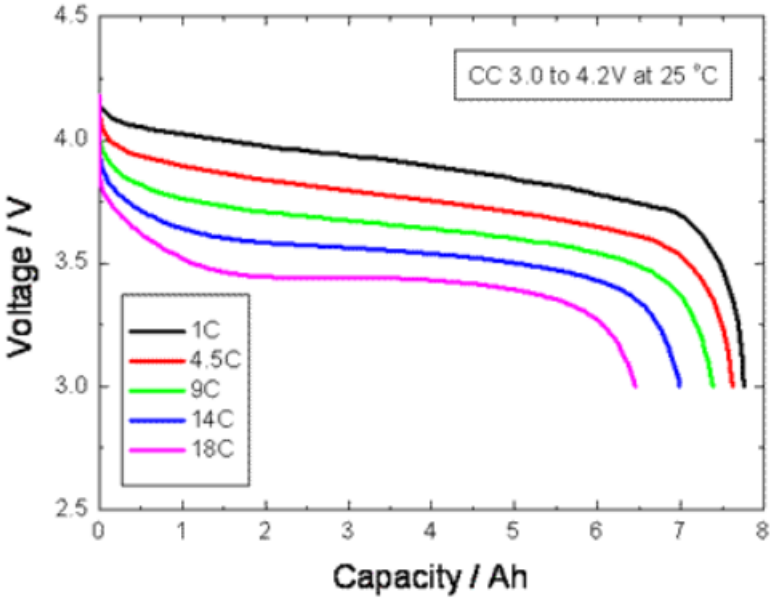

Fig.1.8 Li-ion Discharge rate characteristics

Figure 1.8 shows the discharge rate curves for a Lithium-ion Battery. It states that the productive capacity of the cell is reduced if the cell is discharged at very high rates.

Self-discharge characteristics of the battery are the property of discharging by itself when it is under no use due to the chemical reactions within the cell. This rate of discharge depends on the chemical reactions within the battery and the temperature around it. Lead Acid battery discharges around 4% to 6% per month, and Lithium-ion discharges

around 2 % to 3% per month. The unwanted chemical reactions within the cell increase with the increase in temperature, thereby increasing the self-discharging of the cell.

1.7 DC-DC CONVERTER

DC-DC converter is a device that converts from one dc voltage level to another dc voltage level. There are different topologies available for the conversion from one dc level to another dc level. On the basis of isolation from the mains, there are two types of converters – isolated and non-isolated dc dc converter [20].

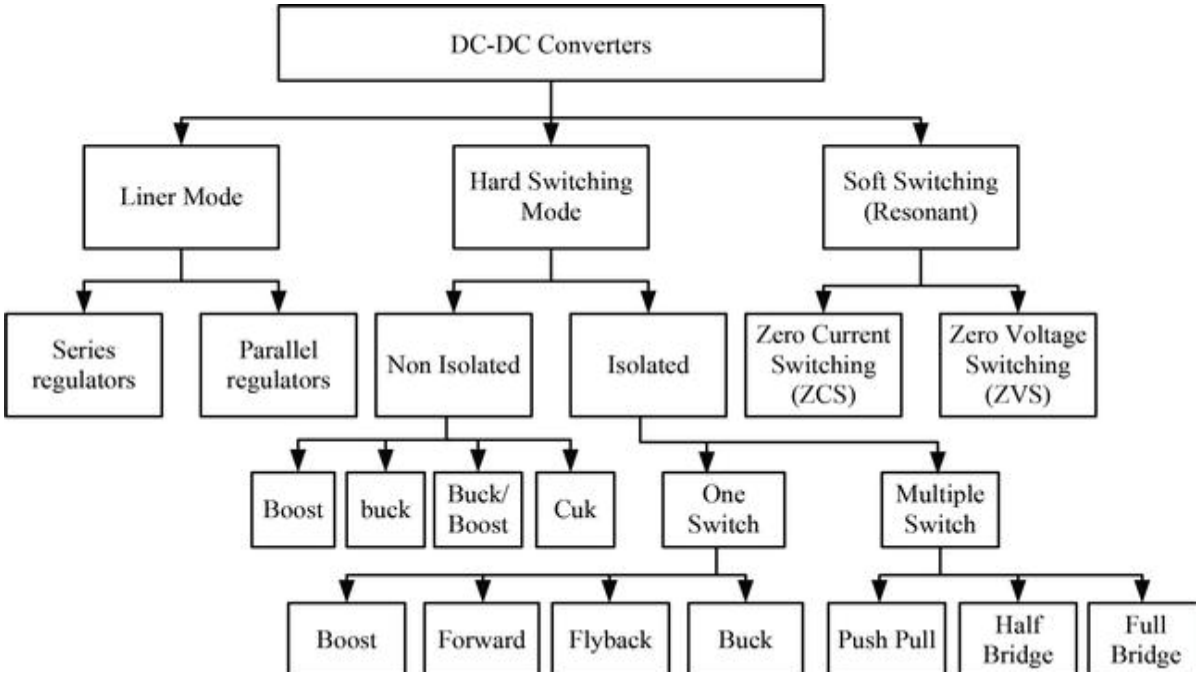

Fig.1.9 Different Topologies of DC-DC Converter

As mentioned, an Isolated converter is one of the topologies so in the case of a full Bridge Converter there is a transformer (provides isolation), dc source, dc output, and filter. If there is a phase shift given to the diagonal switches that is there is a time gap between the diagonal switches turning ON then the Full bridge converter is known as Phase shifted Full bridge Converter.

DC-DC converter should meet some design requirements for automotive applications like high efficiency, small volume, low output current ripple, reject electromagnetic interference, and lightweight.

1.8 OUTLINE OF DISSERTATION

The Dissertation consists of the following chapters:

Chapter 1: It consists of the Introduction for the Thesis where the background of the project has been discussed. It briefs about the charging configuration, and charging power levels for electric vehicles. It introduces the onboard chargers, offboard chargers, unidirectional chargers, and bidirectional chargers. Here, it has also been discussed about battery requirements in EVs along with DC-DC converters and its topologies.

Chapter 2: This chapter consists of the Literature Survey.

Chapter 3: This chapter describes the high-frequency DC-DC Isolated with Rectification and Synchronous Rectification. It contains the MATLAB simulation results and discussions.

Chapter 4: This chapter describes the closed-loop control for the proposed converter for battery charging in electric vehicles. It contains the MATLAB simulation results and discussions

Chapter 5: This chapter concludes the thesis along with the Future Scope.

CHAPTER 2
LITERATURE SURVEY

2.1 SWITCHED-MODE POWER SUPPLIES

Unregulated, linear regulated, and switched-mode power supplies (SMPS) are the three main categories of power supplies. The most basic sort of power supply is an uncontrolled one. Unregulated power supplies, by definition, cannot give a steady voltage like power supplies that are regulated can do. Depending on the output current, the output voltage of the unregulated power supply may vary and produces more ripple. Additionally, the output voltage will likewise fluctuate if the input voltage varies if the input voltage varies, the output voltage will likewise fluctuate. An unregulated power supply is typically pursued by a transistor circuit in a linear regulated power supply circuit which results in achieving a controlled output voltage. Also, linear power supplies have relatively low efficiency because the switch works in the active region. As a result, high-power applications do not use linear voltage regulators. A 99% efficiency can be attained by using an Isolated SMPS with wide-bandgap (WBG) semiconductor devices [21], [22].

With the help of SMPS unregulated DC is converted to a controlled DC voltage. Initially, the AC power is rectified and then filtered. Then, the converter is powered by this uncontrolled DC voltage. This converter must give DC output of the correct level with little AC ripple regardless of changes in the input voltage or the load. Additionally, isolation between the source and the load is necessary for most systems nowadays due to noise and safety concerns. A transformer and an intermediary AC stage are used in SMPS to accomplish this. The converter's switching frequency is typically in the range of hundreds of kHz to avoid bulky magnetic components. The transformer also scales the voltage up or down to reach the best operating point. Switched-mode power supplies as the name suggests use a number of switches that turn on and turn off at high frequency. During the ON state, as shown in Figure 2.1, the switch is in the saturation region, thereby the current flows from drain to source and the voltage drop across the switch is minimum. During the off state, the switch goes in the cut-off region thereby no current flows from the drain to the source. The problem is that as the switch goes into turn-on mode then the voltage across the switch gradually goes to zero due to the parasitic capacitances, hence there exists a short moment of overlapping of current and voltage which is known as switching loss. This

switching loss occurs during the switching on and switching off. This type of switching is also known as hard switching as shown in Figure 2.2. If the switching frequency is high then switching losses is also high. Keeping the frequency high, will surely reduce the size of elements but also increases the switching loss so there exists a comparison between switching power loss and reducing the size of elements to be considered. To have the benefit of both that is reduced switching loss and the device size, soft switching came into the picture.[23]

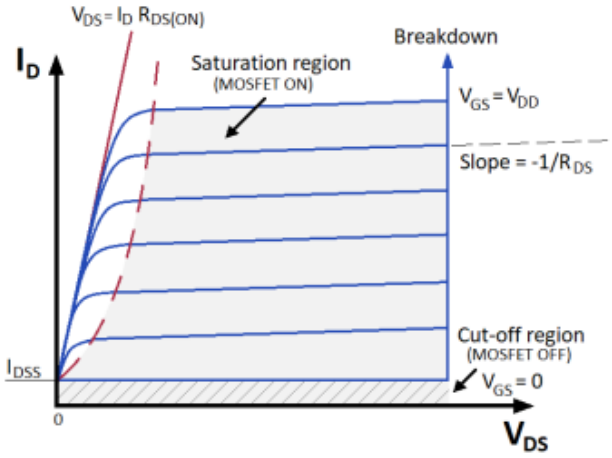

Fig.2.1 Working regions of MOSFET switch

Figure 2.1 shows the different working regions of MOSFET. When the Gate to source voltage is less than the threshold point then the switch works in cut- off region. As the Gate source voltage increases thereby crossing the threshold point then a channel of conduction is formed between the drain and to source. As drain-to-source voltage increases then first it enters a linear region and later after a certain point further increase in the drain-to-source voltage, the drain current does not increase linearly and it saturates at a certain level.

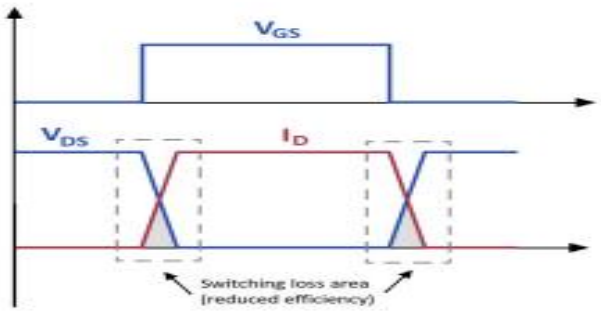

Fig.2.2 Hard switching

Figure 2.2 shows switching where the Drain to source voltage decreases gradually and the Drain current increases gradually, resulting in switching loss.

2.2 SOFT SWITCHING POWER SUPPLIES

Zero current switchings (ZCS) of the power FET are shown in Figure 2.3. This is also true for gate turn-off thyristors (GTO) and insulated-gate bipolar transistors (IGBT), though. When a FET turns on, the drain-to-source voltage drops to almost zero before current flows through its terminals because of the series inductance. As a result, the device's turn-on losses are very low. However, heat will be produced when energy is released from a drain-to-source capacitance. As seen in Figure 2.3, the voltage between the drain and source terminals lowers and reverses upon turn-off. The device is switched off by the reversed voltage, which also causes the current to flow in the other way. Since the device is in the off-state and when voltage is applied again then ideally there should be no turn-off losses. In summary, the ZCS can reduce turn-on losses and eliminate turn-off losses [24],[25].

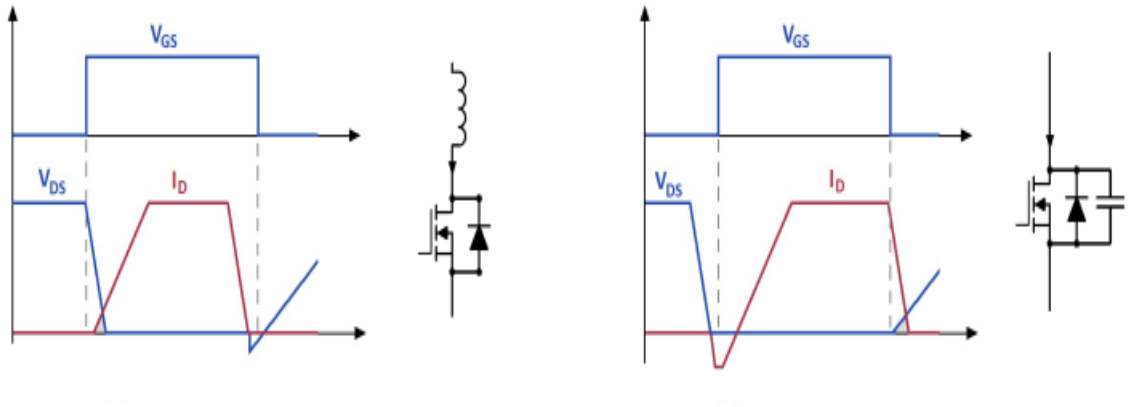

Fig 2.3 Soft Switching Transients

Another soft switching technique is Zero voltage switching (ZVS) where due to the presence of the capacitive element across the power FET device, turn-off losses are decreased. The external resonant circuit decreases the drain to source voltage during turn-on thereby, reducing the turn-on losses during the turn-on transition. Furthermore, unlike ZCS, upon turn-on, the energy of the parallel capacitance is returned to the circuit by resonant action rather than unused in the device. For ZCS circuits, the capacitive turn-on losses are proportional to the switching frequency because they happen every cycle. For higher frequency operations (>100 kHz), ZVS configurations are usually preferred. In the following chapters, the concept of ZVS has been discussed as applied to the selected converter topology [26],[27]. Therefore, it can be said soft switching uses LC resonant circuit for the switching process. It needs more complex circuits to operate the soft-switching technique.

2.3 BRIEF OVERVIEW OF PSFB, DAB, LLC CONVERTER TOPOLOGIES

Here, a brief overview of PSFB, DAB, and LLC converters has been discussed. All these converters belong to the isolated dc converter category. Phase-Shifted Full Bridge (PSFB) and Full Bridge LLC (FB-LLC) are the two primary topologies utilized for high-power DC-DC conversion. These two topologies perform quite well overall and have a component count that is similar. PSFB and DAB belong to the same family where the difference exists only on the working fundamental at the secondary side [28],[29].

2.3.1 FB- LLC converter

The output voltage varies as the switching frequency changes. The gain of the converter is the function of the transformer turns ratio, full bridge gain, and gain of the resonant tank. As the frequency varies, gain also varies.

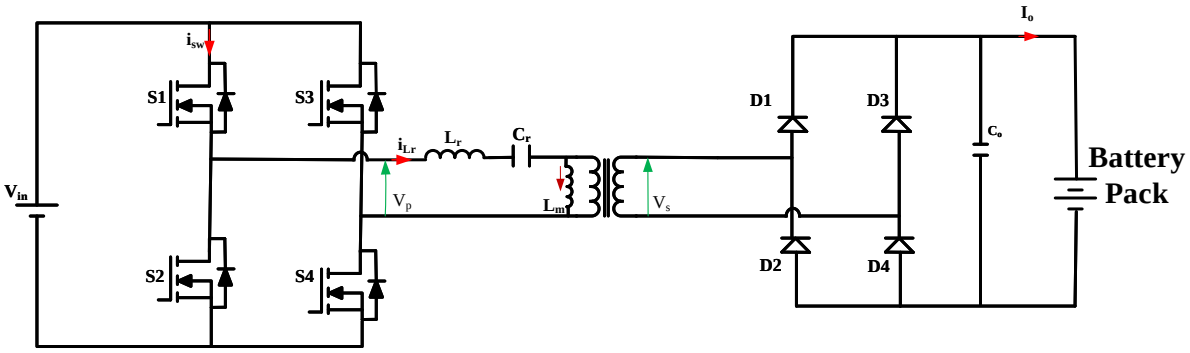

Fig 2.4 Full Bridge LLC converter

Figure 2.4 shows the Full Bridge LLC converter. It consists of:

- Four switches at the primary side for switching and four diodes at the primary side for rectification purposes.
- High-frequency transformer
- A resonant tank circuit of series inductance, and series capacitance. There is the transformer's inductance which is shown parallel to the primary winding of the transformer.
- On the secondary side, the output Capacitor is used as a filter.

In Figure 2.5 it can be seen that Switches S2 and S3 are placed opposite of each other with some dead time to allow for a safe transition, whereas switches S1 and S4 are

controlled by the same control signal [40]. At the full bridge's output, this switching pattern produces a square wave voltage, which is

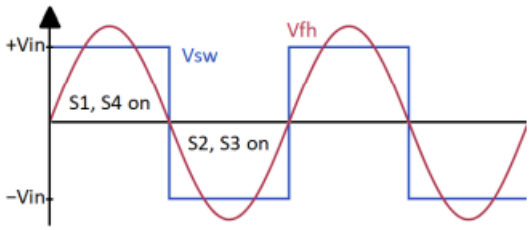

Fig 2.5 Waveform for FB-LLC

then approximated as a sinusoidal waveform using the first harmonic. The gain of the Full-Bridge LLC converter varies with frequency, and the output voltage is regulated by altering the switching frequency.

2.3.2 DAB converter

Wide voltage gain is an added feature in DAB converter which is useful for EV charging applications One of the issues in DAB converter is high frequency current ripple which affects the battery lifetime [30]

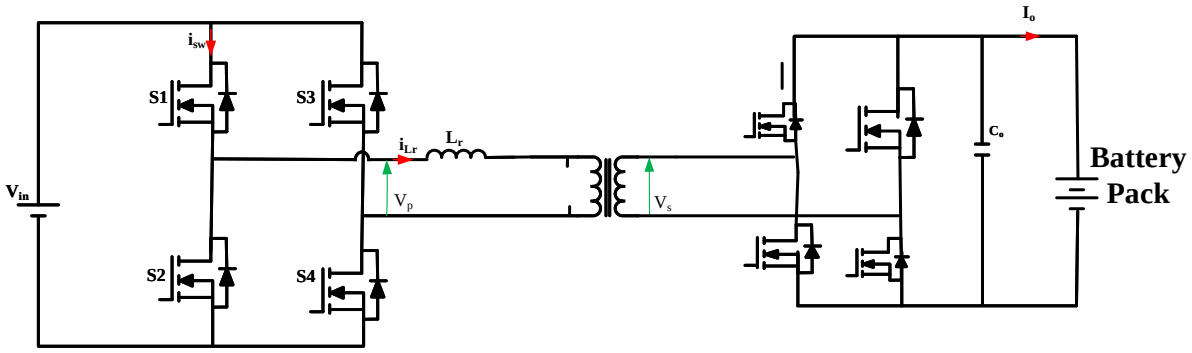

Fig 2.6 Basic configuration of DAB converter

Figure 2.6 shows the basic configuration of the DAB converter. It consists of active switches on both the primary and secondary sides. It supports inherent switching, provides galvanic isolation, and high voltage ratio gain. The phase shift exists between the diagonal switches of both bridges which allows the power flow.

2.3.3 PSFB converter

Due to its outstanding features including soft-switching capability of the major active switches, straightforward PWM control with a constant frequency, flexibility, reduced current load on the devices, and low EMI, PSFB has demonstrated its promise for

EV chargers. The variation in phase between diagonal switches at the primary side causes the power flow.

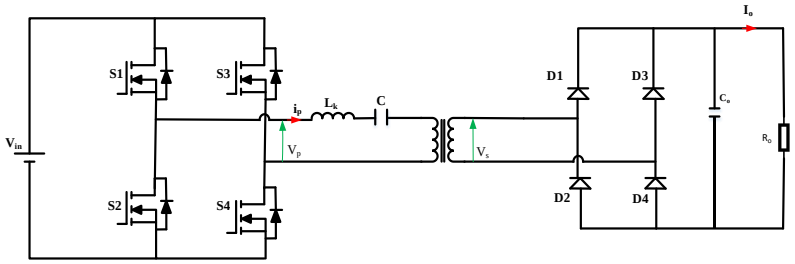

Fig 2.7 Phase- shifted full bridge converter

Figure 2.7 shows the PSFB converter. It consists of four semiconductor switches at the primary side with body diodes along with four diodes at the secondary side. A separate inductor along with the transformer's leakage inductance can also be used for operation of the PSFB converter. In the figure, the high-frequency transformer and at output side capacitive filter is shown.

TABLE 2.1 Comparison of FB-LLC, DAB, PSFB converter

Factors	**FB-LLC**	**DAB**	**PSFB**
Output Capacitor	Large capacitor, very high ripple	High ripple	Low ripple
Output Inductor	Not used	Not used	Used
Soft Switching	ZVS, but difficult at higher frequency	ZVS is possible for all primary and secondary side switches.	ZVS
Output voltage range	Medium	Can achieve wide range of output voltage with no trade-off with efficiency	High range of output voltage
Control	Frequency control	Phase shift control	Phase shift control

2.4 RECTIFIER STATE TOPOLOGY

Different rectification topologies have been discussed in this section. Full bridge rectifiers, centre-tapped rectifiers, synchronous rectification, and diode rectification has been covered in this section.

2.4.1 Centre-Tapped Rectifier and Full bridge rectifier

In Figure 2.8, there are two full-wave rectifier topologies. The difference between the two is that one employs a centre-tapped transformer and two semiconductor devices, while the other a conventional transformer and four semiconductor devices. Only one of the secondary windings is ever conducting in a centre-tapped rectifier. As a result, the transformer will be larger. In addition, compared to a bridge rectifier, the reverse voltage applied to diodes will be two times higher [31],[32].

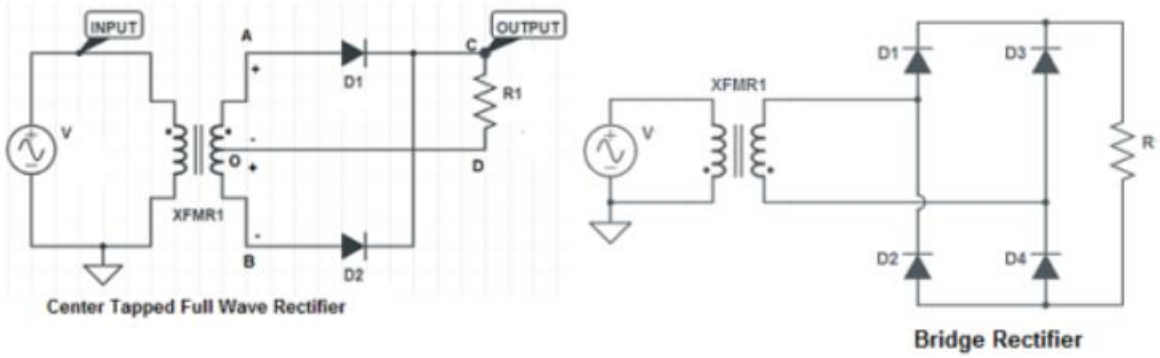

Fig.2.8 Centre-tapped rectifier and Bridge Rectifier

Also, the bridge rectifier case has a larger transformer utilization factor (TUF). The centre-tapped rectifier has the advantage of having two rather than four semiconductor components. This has economic implications, but it also means that there will be a voltage drop over just one item connected to the output in series. Consequently, it is more effective.

2.4.2 Synchronous Rectification and Diode Rectification

The most popular and straightforward rectification method utilised in medium- and high-power applications is the diode rectifier. Robustness and ease of use are the key benefits of employing a diode rectifier. However, the efficiency of the system is impacted by the lower limit of 0.3V for voltage drop over a diode.

MOSFETs are used in synchronous rectification in place of diodes as shown in Figure 2.9. Lowering the drain to source resistance helps reduce the voltage loss over

MOSFETs. So synchronous rectification may be more effective for some current levels. However, there are now two additional gate drive circuits and the control is more complex.

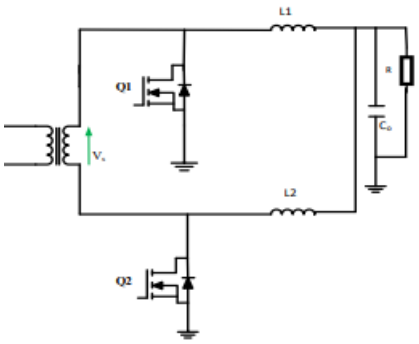

Fig.2.9 Synchronous rectification

Only changing the rectifier module is necessary to accomplish synchronous rectification.

2.5 ZERO VOLTAGE TRANSITION

In this section, zero voltage switching has been discussed. Fundamentally, ZVS was accomplished by charging and discharging capacitors with the help of the energy held in the shim inductor during this brief transient period. Consequently, two requirements must be fulfilled in attempt to attain ZVS. The inductor's energy must first be sufficient to either charge or discharge the upper and lower capacitors on the same leg. Second, the completion of this transient is required before the FET is given the turn-on signal. Total equivalent capacitance is given by equation 2.1

$$C_{total} = C_c + C_D + C_{tr} \tag{2.1}$$

where, Ctr is transformers parasitic capacitance , Cc & Cd are parasitic capacitances of switches. So the total energy required is

$$W_{capacitive} = \frac{1}{2} C_{total} * V_{in} * V_{in} \tag{2.2}$$

The energy stored in leakage inductance of transformer is

$$W_{inductive} = \frac{1}{2} Ls * (I_{primary})^2 \tag{2.3}$$

The first condition is expressed as :

$$W_{inductive} > W_{capacitive} \tag{2.4}$$

To satisfy the first condition inductance is added at the primary side of the transformer to supply the energy for achieving ZVS at different load conditions.

In order to allow for the whole transient, the second criterion requires that the delay period before turning on the FET be precisely determined. One method to do it is as given in equation 2.5

$$t_{delay} = \frac{k}{4 * f_{res}} \tag{2.5}$$

In equation 2.5, resonant tank frequency f_{res} is given by equation 2.6

$$f_{res} = \frac{1}{2 * \pi * \sqrt{Ls * C_{out}}} \tag{2.6}$$

Based on the empirical data, the coefficient k in equation 2.6 is 1 in or increased up to 2.25 in. In any event, this delay time is only an estimate, and the actual transient time will vary depending on the load circumstances. Consequently, a number of research have been conducted to investigate the possibility of adaptive dead time, and certain control circuits offer a programmable adaptive delay function. It is possible to obtain the necessary amount of primary current by a number of methods. Limiting the minimum load current to the proper level is the simplest strategy [33].

However, designing the transformer's magnetizing inductance appropriately provides an alternative. The reflected secondary inductor current contribution, which is modelled in parallel, contributes to the magnetizing current as well. It is also necessary to consider any duty cycle changes that can affect the peak charging current. In many off-line high-frequency converters, the magnetizing current alone is usually not enough. Since the transformer's core loss is often constrained, it has many primary turns and a large magnetizing inductance. One option to generate the appropriate amount of primary current is to shunt the transformer primary using an external inductor. Another option is to use the output filter's magnetizing current to aid resonance on the primary side.

With the dissipative discharge of the FET output capacitance, switching losses caused by the simultaneous overlap of voltage and current disappear. Due to the "soft" switching characteristics, which advantageously include parasitic components of the power stage, EMI/RFI is greatly reduced [34].

2.6 SMALL SIGNAL MODEL OF PSFB

The process of creating a mathematical description of a system can be referred to as modeling the system. It involves creating a mathematical input-output model that most closely resembles a system's physical reality. Systems using switching converters are nonlinear. The switching converter model is linearized since the system must be linearized in order to analyze such converters. Such a linearized model has the benefit of being time-invariant for a constant duty cycle. Only the DC components of the waveforms are represented, thus switching and switching ripple has no concerns.[35]

Modelling the behaviour of a dynamic converter is required in order to build the converter's control system. Unfortunately, the switching and pulse width modulation processes' nonlinear time-varying nature makes it difficult to figure out the dynamic behaviour of converters.

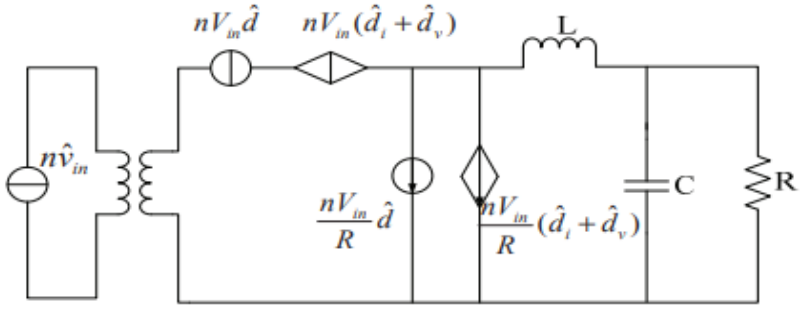

Fig. 2.10 The small signal model of PSFB

In Figure 2.10 the small signal model of PSFB has been shown which is a buck-derived topology. Any switching DC-DC converter needs to be controlled in a closed loop, hence modeling the converter's small signal model (SSM) is necessary. We may obtain entire transfer functions for the supplied DC-DC converter via small signal analysis. Additionally, small signal analysis aids in locating the deviation from the steady state operating point, which reduces ripple and helps in attaining consistent and controlled output voltage. According to Figure 2.10, for the open loop control duty cycle to Output transfer function is given by Equation 2.7

$$G_{vd} = \frac{(Ns/Np)*Vin}{s^2 L_o C_o + s\left(\frac{L}{R_{load}} + R_d C\right) + \frac{R_d}{R_{load}} + 1} \tag{2.7}$$

where,

$$R_d = 4 * (\frac{N_s}{N_p})^2 * f_{sw} * L_s \quad (2.8)$$

The PSFB DC/DC converter's small-signal circuit model and the buck converter's small-signal circuit model are extremely similar. However, there are still distinctions between the two categories of small-signal circuit models. Because the PSFB converter's dynamic properties are significantly impacted by the duty cycle loss.

CHAPTER 3
HIGH-FREQUENCY DC-DC ISOLATED CONVERTER WITH RECTIFICATION AND SYNCHRONOUS RECTIFICATION

3.1 INTRODUCTION

. A DC-DC converter steps up or step down the voltage level depending on different applications. A typical electric vehicle (EV) powertrain is composed of several power electronics converter subsystems. Depending upon safe charging, DC-DC converter topologies are isolated and non-isolated dc-dc converters. When it comes to isolated topology then full-bridge configuration is most frequently implemented as it is suitable for high power transmission due to its characteristic feature of ZVS and switches working at high frequency. A high-frequency transformer is often used in isolated dc-dc converters. The use of high-frequency transformers makes the isolated converter different from the non-isolated converter which adds benefits to the isolated topology. Due to their compact size, high-frequency transformers can ignore undesirable characteristics including inductance leakage and eddy current losses [36]. To avoid bulky components. Since transformers need an AC supply, an inverter is required to convert dc into ac which is facilitated by the proposed full-bridge dc-dc converter.

Switching losses, poor efficiency, and voltage spikes are caused by oscillations at conventional FB-type converters between the parasitic capacitors of the power components and the leakage inductance of the transformer. To achieve Smooth Switching, the phase-shift control approach is used. A synchronous rectification at the secondary side enhances the efficiency further for the PSFB converter. The two MOSFET switches make the circuit more complex to control in the case of synchronous rectification [37],[38]. PSFB converter consists of three stages of power flow. The first stage is input dc then the second stage is dc to ac which is fed to the high-frequency transformer and later the third stage is ac to output dc which is fed to the load. For medium and high-power applications, PSFB converters are one of the most used dc/dc converters. Due to the soft switching capability of the major active switches, PWM control with a constant frequency, wide range, reduced current stress on the devices, and low electromagnetic interference, PSFB has come up for EV chargers. The phase shift between the diagonal switches affects the PSFB's output power. When the phase shift is zero, the duty cycle is 1, which causes the converter to operate in hard-switched mode [39]. When the phase-shift angle is equal to 180 degrees,

there is no power transmission and the duty cycle is zero. Soft switching is the alternative to hard switching. If the current or voltage is zero during the transient in the MOSFET switch, the soft switching is visible [40]. Zero current switchings (ZCS) and zero voltage switching are two soft switching techniques (ZVS) [41]. Here in this chapter, ZVS has been implemented resulting in minimum switching losses. Electric vehicle loads ranging from 600 W to 3.3 kW can be handled by PSFB with ZVS architecture [42].

3.2 PSFB WITH RECTIFICATION AND SYNCHRONOUS RECTIFICATION

The phase-shifted PWM complete bridge converter is a two-stage device. To enable ZVS transition and make sure that the primary winding is shorted or connected to the input, the control signal to switches S3 and S4 is phase-shifted with regard to the gating signal to switches S1 and S2. It has also to be ensured that at no point in time, dc supply is shorted. The diode on the secondary side aids in rectification. Both center-tapped and full-bridge rectifiers, which use diodes, can be used for rectification. Synchronous rectification is a technique for rectification, in which MOSFETs are employed in place of diodes. By reducing the drain to source resistance while the MOSFET is ON, the voltage drop across the device can be reduced. Therefore, synchronous rectification may be more effective at some current levels. However, there are now two additional gate drive circuits and the control is more intricate. For simple control, full-wave diode rectification is utilized.

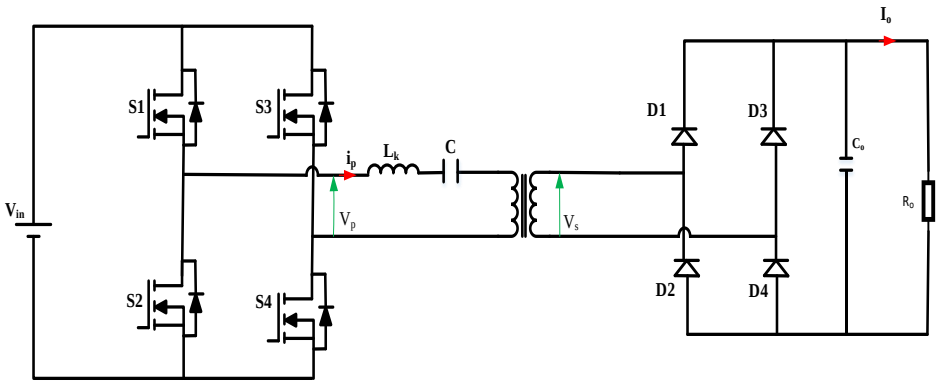

Fig.3.1 Phase Shifted Full Bridge Converter

Figure 3.1 depicts the structure of the ZVS phase-shift full bridge PWM converter, which differs from ordinary full bridge converters by having four switching elements and switching control signals.

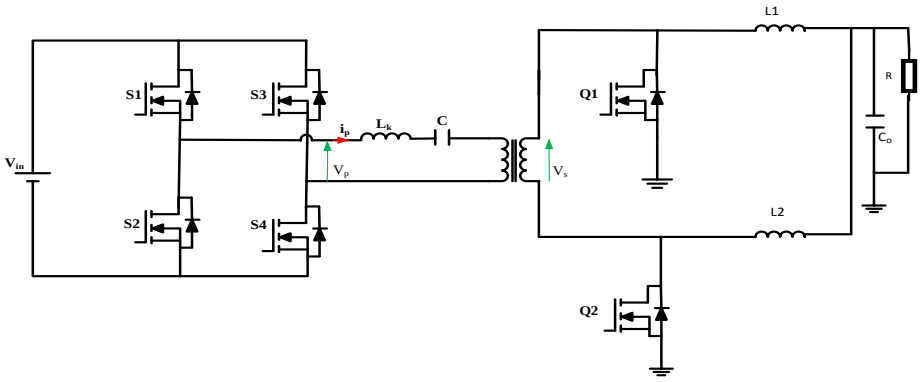

Fig.3.2 PSFB with Synchronous Rectification

Here, the secondary side diodes have been replaced with Mosfet switches. The optimum value of R_{dson} for Mosfet will help in minimizing the switching losses. The two Mosfets are controlled by a pulse generator and help in completing the path for circuit operation at the secondary side. Fig. 3.2 shows PSFB with Synchronous Rectification where two MOSFET and two inductors are present at the secondary side. The controlling of the switch at the Secondary side plays a key role.

3.3 DESIGN AND ANALYSIS

This section covers the design and analysis of the proposed converter. It describes the conditions for attaining ZVS and later, the design specifications has been mentioned.

3.3.1 Analysis of ZVS

By utilizing the energy stored in the transformer's leakage inductance to discharge the switches' output capacitance before turning them on, the Zero Voltage Turn ON is made possible. The energy stored in the leaking inductance must be greater than the energy stored in the output capacitances in order to accomplish ZVS.

$$E = \frac{1}{2} L_{lk} I^2 > \frac{4}{3} C_{MOS} V_{in}^{\ 2} + \frac{1}{2} C_{tr} V_{in}^{\ 2} \qquad (1)$$

where, C_{MOS} is the output capacitance of the switch

C_{tr} is the transformer winding capacitance

Consequently, in order to attain the ZVS, two key requirements must be fulfilled. Energy in the inductor must be enough to charge and discharge the capacitor. Second, the transient should over before the switch gets ON.

For simplification, the above equation can be written as:

$$\frac{1}{2} L_{lk} I^2 > \frac{1}{2} C_{eq} V_{in}^{\ 2} \qquad (2)$$

where C_{eq} is the equivalent capacitance

I is the primary current

On solving further input primary current can be written as:

$$I = \sqrt{\frac{C_{eq} * V_{in}^2}{L_{lk}}} \quad (3)$$

3.3.2 Design Specifications

TABLE 3.1 **Lists the specifications for a PSFB converter**

Parameters	**Unit**	**Values**
Input voltage	V	380
Output voltage	V	72
Switching frequency	kHz	200
Output current ripple	%	20
Output voltage ripple	%	40
Power Rating	kW	1.1

Choosing the duty ratio as *50%* and using the above design specifications, turns ratio N is calculated as:

$$N = \frac{(V_{in} - 2V_{rdson})D}{V_o + V_d} \quad (4)$$

In equation (4) above V_{rdson} is a voltage drop over the MOSFET and V_d is a voltage drop across the rectifier diode.

Since the output inductor ripple current is limited to 20%, so ΔIL can be calculated as:

$$\Delta I_L = \frac{P_{out}}{V_s} * 0.2 \quad (5)$$

The magnetizing inductance of the primary transformer is calculated as:

$$L_{mag} = \frac{V_{in}(1-D).N}{\Delta I_L.P_{out}.0.5} \quad (6)$$

The output filter inductor is given by:

$$L = \frac{V * D}{I * f} \quad (7)$$

The output filter capacitor is given by:

$$C_{out} = \frac{I_{ripple} * D}{V_{ripple} * f_s} \quad (8)$$

3.4 MATLAB SIMULATION RESULTS AND DISCUSSIONS

The results for the PSFB DC-DC Converter have been obtained at a switching frequency of 200 kHz with input Voltage 380 V, Output Voltage 72 V, and later the results have been obtained for PSFB with synchronous rectification.

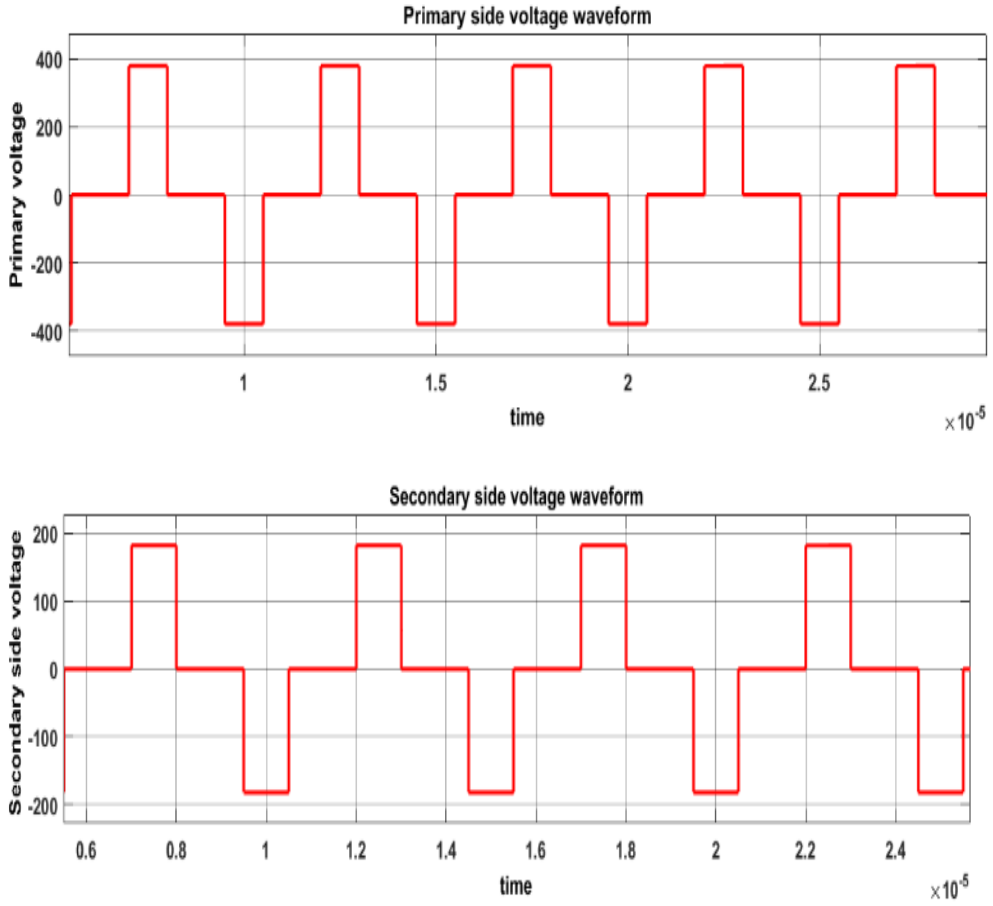

Fig. 3.3 Primary and secondary side voltage waveform

In Figure 3.3, the primary and secondary side voltage waveform has been shown. At the gate of the MOSFET, a pulse generator has been applied. With the help of a pulse generator square-shaped pulse of frequency, 200 kHz has been given to all four switches. A shift in the pulse between Diagonal switches has been maintained. With S_1, and S_4 ON the transformer is energized from the DC source and similar happens when S_4 and S_3 are ON, hence resulting in a Quasi square wave. The phase shift is given such that at any point in time two switches are operational. When S_1 and S_3 are ON for a short duration then, the primary of the transformer shows zero voltage across it which can be observed in figure 3.1 The phase shift between diagonal switches that is the starting time of conduction for diagonal switches varies by short duration. Thereby, the DC input to the transformer's primary winding varies accordingly.

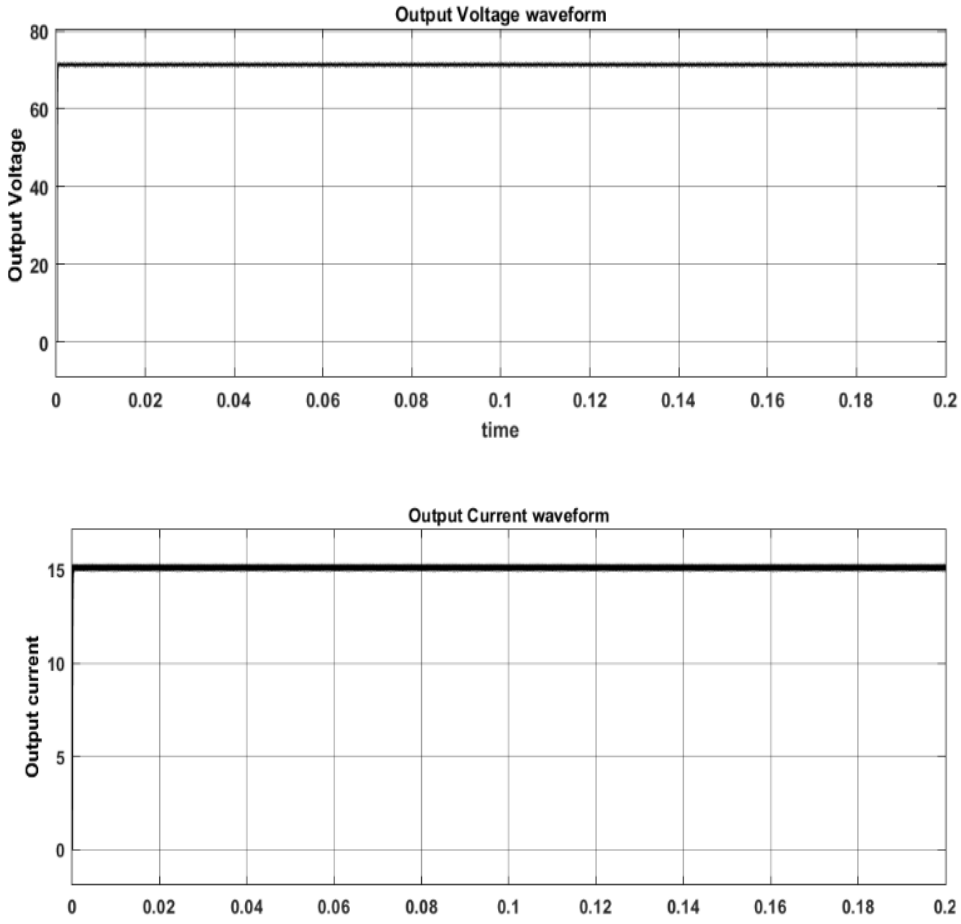

Fig. 3.4 Output Voltage and current waveform

In Figure 3.4, the output voltage and current waveform have been shown. The output of the transformer's secondary is fed to the full bridge rectifier which helps in attaining DC values. These DC quantities are passed through an LC filter at the output which improves the quality of the DC quantities and also gives gain for the circuit. Hence, on the output side, we are able to achieve the given specification values which fulfill the sole purpose of the given DC-DC converter. The output voltage achieved is 72 V and the output is 15 A.

In Figure 3.5, pulse generator waveforms have been shown. It can be observed from the figure that a pulse of constant amplitude, has been fed to the Gate of the MOSFET which controls the switch. A phase shift can also be observed between the diagonal switches that are S_1 - S_4, and S_3 - S_2. S_1 and S_4 conduct at a time than S_3 and S_2 conduct at a time. For a short duration, there is a common point of contact for S_1 and S_3 resulting in almost no voltage across the Transformer and the same happens for switches S_2 and S_4 also.

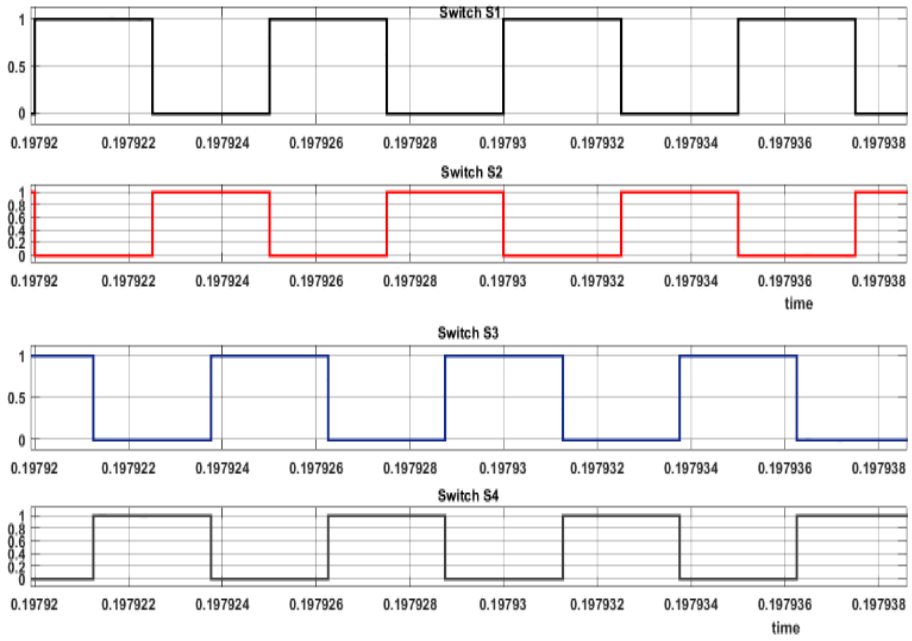

Fig. 3.5 Switching pulse waveforms

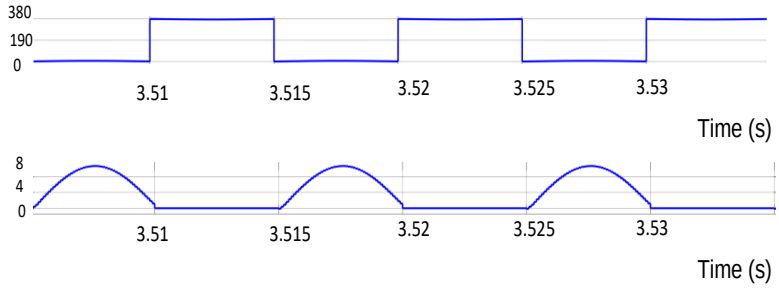

Fig.3.6 ZVS across Switch S1

In Fig. 3.6, Zero Voltage Switching has been shown across Switch S_1. It can be observed that voltage across the switch is zero that is the inductive energy of the leakage inductor that has discharged the snubber capacitance of the switch then the switch starts conducting hence resulting in zero switching loss. It can also be observed across the other three switches also. The leakage inductor is a key element that controls the ZVS transitions.

TABLE 3.1 Lists the efficiency for different values of load current for diode rectification

Load (%)	**Efficiency (%)**
Full load	92
80	90
50	87
30	80.56

PFSB with Synchronous Rectification:

Here, on the secondary side, two MOSFET switches have been used for the purpose of Rectification and two inductors have been connected at the load side for the splitting of the current into two parts. The control of the two MOSFETs at secondary is complex but it is efficient for the system. Fig 3.7 shows the Primary and Secondary Voltage waveform across the transformer's primary winding.

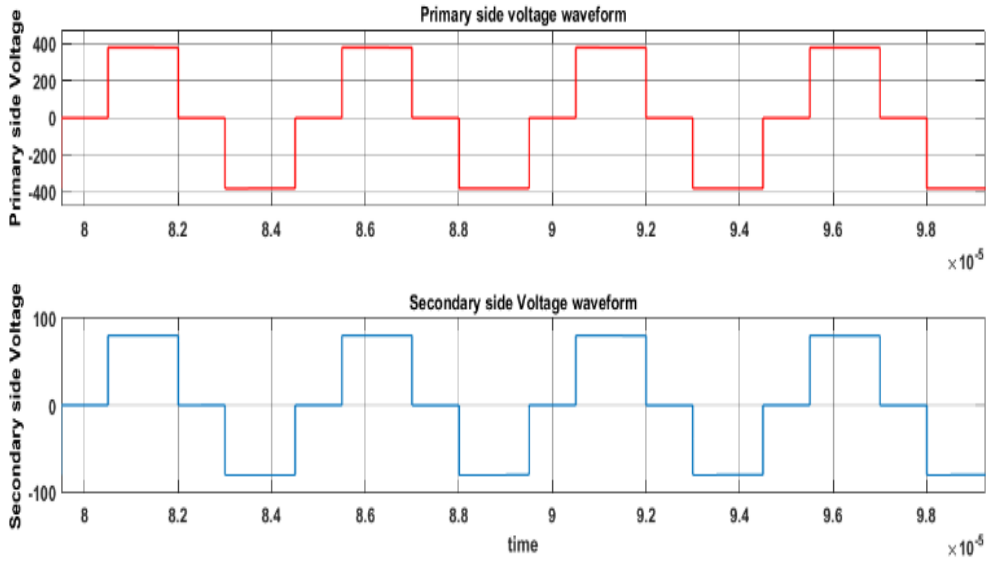

Fig. 3.7 Primary and Secondary voltage waveform across the transformer

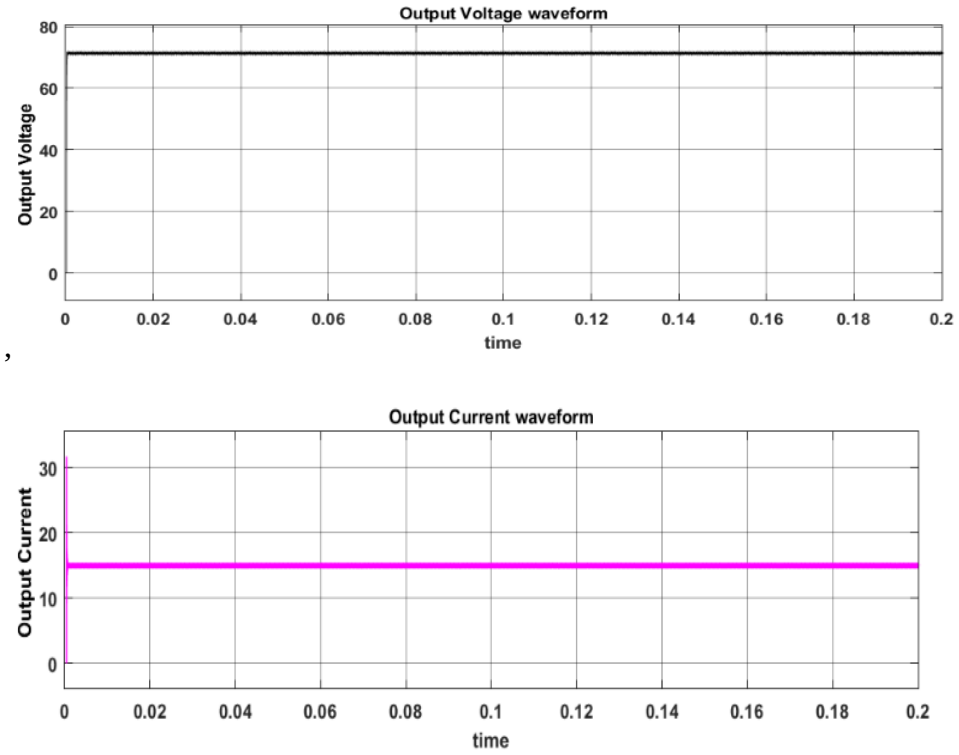

Fig 3.8 Output Voltage and Current waveform at the Load side

Fig.3.8 depicts the Output voltage and output current waveform at the Load side operated for Synchronous Rectification. The secondary side is connected to the Synchronous rectifiers thereby reducing switching power loss and improving heat dissipation. At a different value of load conditions, the magnitude of voltage and current will be different.

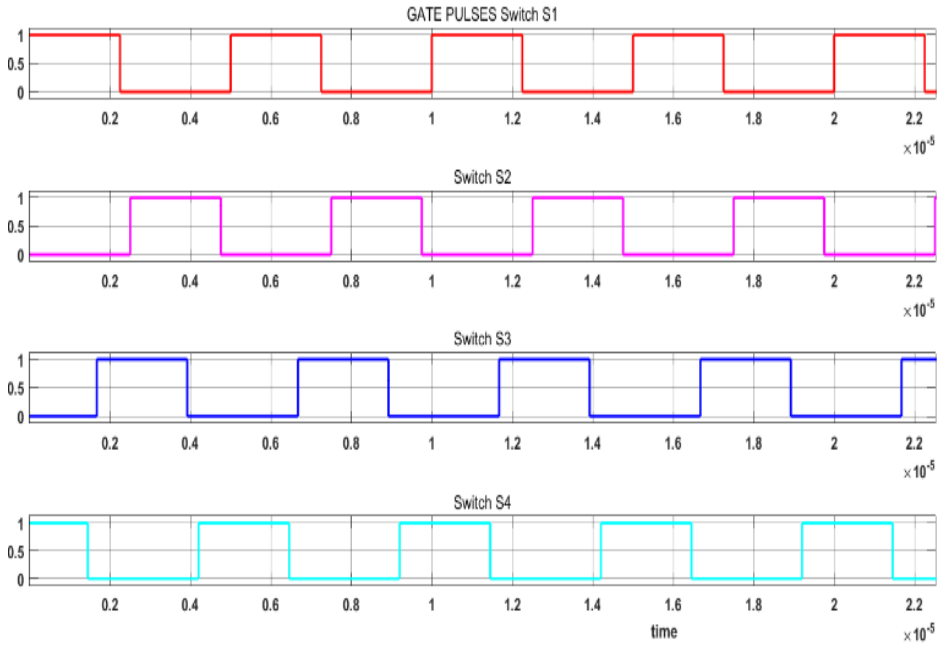

Fig 3.9. Switching pulse waveforms applied to switches *S1, S2, S3, S4*

In Figure 3.9 Switching pulse fed to switches at the primary side is depicted. The phase shift has been maintained across Diagonal switches.

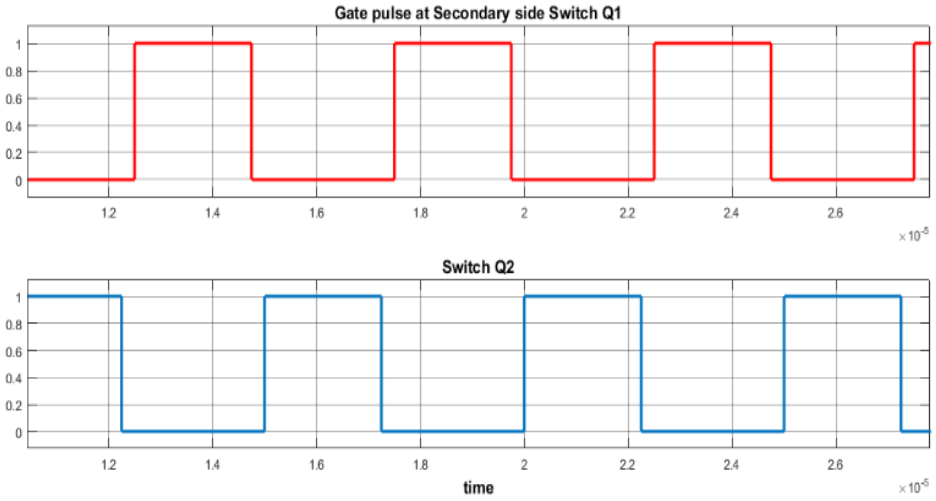

Fig. 3.10 Switching Pulse at Q1 and Q2

In Fig. 3.10 The switching pulse at Q_1 is the same that as fed to S_2 and the switching pulse at $Q2$ is the same as that fed to S_1. Switches Q_1, and Q_2 are at the secondary side thereby helping in completing the path at the load side

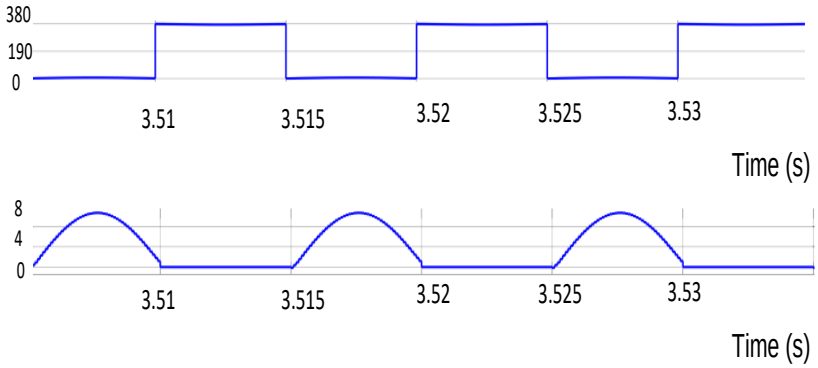

Fig.3.11 ZVS across switch S_1

In Figure 3.11, it shows the switches attaining ZVS as it can be observed that at zero voltage across Switches, the turn-on process occurs. At the secondary side current splits into two different paths and hence, conductivity losses reduce. If the drain-to-source resistance is reduced then the Voltage drop across the switch is low.

TABLE 3.2 Lists the efficiency for different values of load current for synchronous rectification

Load	**Efficiency (%)**
Full load	95
80 % of the full load	93.20
50 % of the full load	90
30% of the full load	86

At a different load value, the converter has been analyzed thereby, efficiency has been calculated for different values of load current

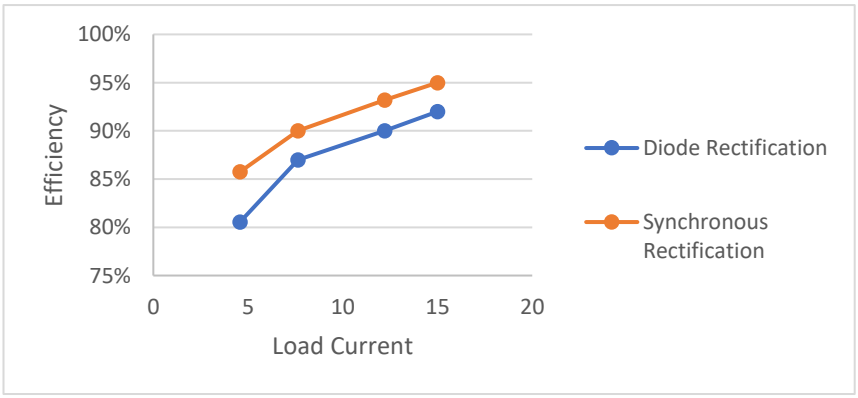

Fig 3.12. Load Current vs Efficiency for PSFB

Fig 3.12 shows the variation of Efficiency as the load current is varied. The load current has been calculated at different values of R-load

TABLE 3.3 Lists the comparison for diode rectification and synchronous rectification

PSFB with diode rectification	**PSFB with synchronous rectification**
Diode's forward voltage drop is more	MOSFET R_{ds} (resistance across drain to source) ON will be less.
The switching speed is normal	Better switching speed
Conduction losses is more.	MOSFETS can be paralleled to have fewer conduction losses

3.4 CONCLUSION

A 200 kHz switching frequency ZVS PSFB dc-dc converter and PSFB with Synchronous Rectifier have been Modeled in the Simulink environment. PSFB is preferred in EV battery charging applications and it supports ZVS over a wide load range. It is more efficient to run PSFB with Synchronous Rectification for higher efficiency. PSFB with synchronous rectification is preferred over conventional PSFB. It is to be noted that MOSFET output capacitance should be kept low in order to extend the ZVS range. The model was analyzed under various loading conditions. Synchronous Rectification was able to deliver 95% efficiency at full load which was found to be better than conventional PSFB.

CHAPTER 4
CLOSED-LOOP CONTROL OF DC-DC ISOLATED CONVERTER FOR EV BATTERY CHARGING

4.1 INTRODUCTION

There are different topologies available in DC-DC converters as per the requirement of voltage levels and efficiencies. Based on safety and galvanic isolation DC converters are classified as Isolated converters and non-Isolated converters. Isolated converters use high-frequency transformers and provide galvanic isolation. Converters like LLC, and DAB come under this category. Some examples of non-isolated converters are Buck-Boost converters, flyback converters, and CUK converters [43]. The basic stages of charging are from ac (from the grid) to dc and then dc to dc conversion. Onboard EV chargers directly take ac from the supply and the later stages of conversion ac to dc and then dc to the required dc for the battery is present inside the vehicle charging system whereas, in Offboard chargers, DC is directly fed to the vehicle battery system, where DC-DC conversion occurs where DC-DC converters play a vital role in charging. The working of the converter also influences the lifetime of the battery [44]. Both ac and dc charging is possible; ac charging often specifies level 1 and level 2 onboard chargers whereas dc charging is specified by level 3 off-board chargers. Level 1 is simple charging available at residential, buildings where 230V ac is available. It supports 12 A to 15 A of current (Single Phase). Level 1 charging is slow charging. Level-2 ac chargers can produce up to 20kW of power and are typically utilized in commercial locations like malls and workplaces. Modern Level-2 charging stations accept 208Vac or 240Vac as input voltage. Level 3 chargers are fast offboarding DC-DC chargers. Figure 4.1 shows the stages of the charging system. It depicts the power level conversion stage [45],[46]

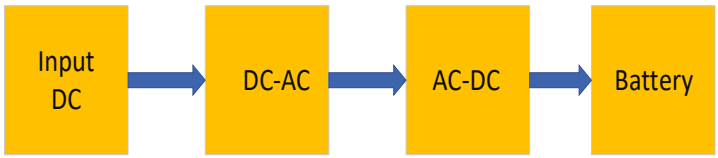

Fig.4.1 Stages of conversion

PSFB with synchronous rectification is a good selection for EV chargers as it has the soft-switching capability, low stress on switches, low and EMI, simple PWM control. It has high efficiency and a wide range of ZVS than the conventional PSFB with diode rectification. It allows working at high frequency resulting in high power density. The closed loop PI

control has been used to achieve CC mode charging. The PI controller controls the pulses which is fed at the MOSFET switches [47],[48].

4.2 DESIGN AND ANALYSIS OF THE BATTERY CHARGING SYSTEM

The block diagram of the proposed charging consists of Input dc, dc-ac conversion, ac-dc conversion, Battery, and CC controller. Input DC is fed to the Phase shifted full bridge converter which is then converted to the EVs battery voltage level. AC power from the grid can be rectified to DC and fed at the input DC level. Other forms of renewable energy like solar energy can be used to feed power at input DC. In the Block diagram, different stages have been shown under the block Phase shifted Full bridge Converter. The first stage is DC to AC conversion with the help of the H bridge structure present in PSFB. This ac is fed to the high-frequency transformer which stores energy in the form of magnetic energy and builds the voltage level. In the last stage, this ac is converted to dc with the help of synchronous rectification where two MOSFETs are used at the secondary side of the high-frequency transformer. Here, Synchronous Rectification helps in attaining the dc voltage level at high efficiency. This dc is passed through the LC filter.

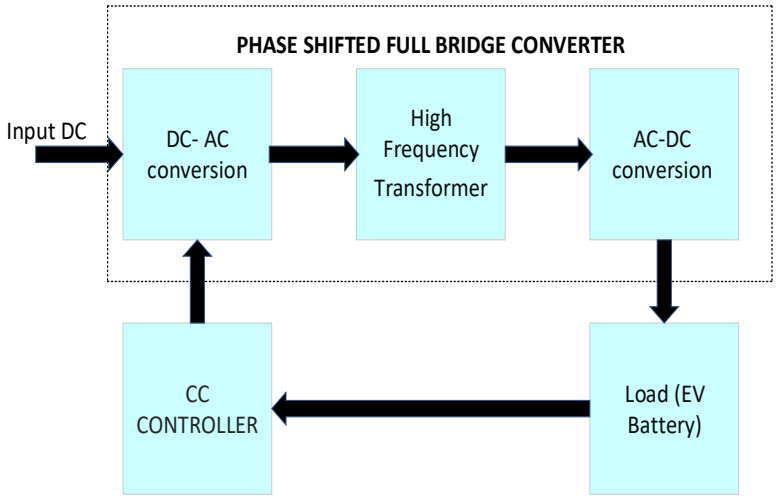

Fig.4.2. Block diagram of Proposed Charging System

With the help of an LC filter, the output dc current and voltage smoothen, thereby, feeding better quality charging current to the battery. Figure 4.2 shows the Block diagram of the proposed Charging system. The CC controller consists of a PI controller which helps in maintaining the constant required current to the battery and also protects the battery from overheating. The output voltage obtained at the secondary side of the converter should be greater than the battery nominal voltage for better and more efficient charging [51],[52].

4.2.1 PI controller design and Operation

The closed-loop control of the battery charging current is done using a PI(also, known as Proportional Integral) controller. PI controller is a feedback control loop that helps in setting the desired value at the output. The reference desired value is set and with the help of the sensor, the output charging current of the battery is sensed. The difference between the reference value of the current and the output charging current known as the error signal is fed to the PI controller. This helps in controlling the switching pulses given to Switches, thereby controlling the operation of switches accordingly and helping to achieve a uniform charging current for the battery [49],[50]. The mathematical equation of the PI controller is given by:

$$u(t) = k_p e(t) + k_i \int_0^t e(t)dT \qquad (1)$$

where, u(t) is the controlling signal, e(t) is the error signal
k_p is the proportional gain constant of P -term
k_i is the integral gain of I-term
The combination of proportional and integral signals is known as the controlling signal u(t). The setting of K_p and K_i is important for tuning the PI control and hence achieving the desired charging current at the battery side

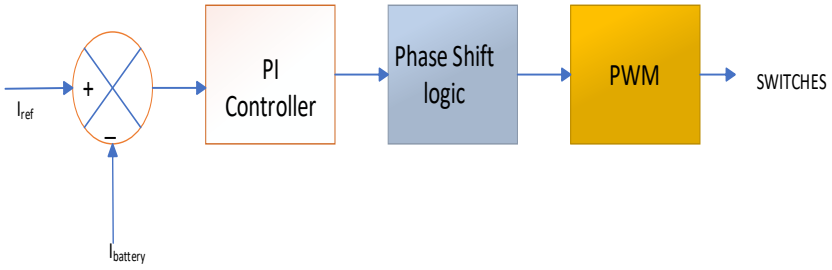

Fig.4.3 Block diagram of PI control strategy

Figure 4.3 shows the block diagram of the PI control strategy. The diagram states the control of the charging current. of the battery. The PI controller helps in improving steady-state error characteristics for the system.

4.2.2 Design of filter and design specifications

The capacitor inductor filter at the output side is designed using the following equations. The voltage drop across the output inductor is given as

$$V_L = V_{in}\frac{N_s}{N_p} - Vo \quad (2)$$

V_o is the output voltage

$V_{in}\frac{N_s}{N_p}$ is the secondary side transformer voltage with turns ratio N_s/N_p

$$V_L = \frac{di}{dt} \quad (3)$$

Using equations 1 and 2 , the inductance L can be written as

$$L = V_L\frac{DT_s}{I_{ripple}} \quad (4)$$

The output current through the filter capacitor is given as

$$I_{ripple} = C\frac{dv}{dt} \quad (5)$$

Equation 4 can be further written as

$$C = I_{ripple}\frac{DT_s}{V_{ripple}} \quad (6)$$

TABLE 4.1 Lists the system parameters

PARAMETERS	**UNITS**	**VALUE**
Input voltage	V	380
Output voltage	V	55
Switching frequency	kHz	200
Output current ripple	%	20
Output voltage ripple	%	40
Power rating	kW	5.5
Battery nominal voltage	V	48
Battery Ah rating	Ah	100
Battery Initial SOC	%	40

Depending on the requirement, batteries can be charged at different rates. Appropriate safety measures must be taken in order to maximize the charging rate, ensure the battery is fully charged, and prevent overcharging therefore, the system is operated under CC mode to charge 48V,100Ah battery.

4.3 MATLAB SIMULATION RESULTS AND DISCUSSIONS

The MATLAB Simulink environment is used to model the proposed charging system. The model consists of, a PSFB DC-DC converter, a PI controller, Lithium Ion Battery. The input DC voltage is 380 V, the output at the converter is 55 V, Switching Frequency is 200 kHz is used to charge a 48 V, 100 Ah Lithium-ion Battery.

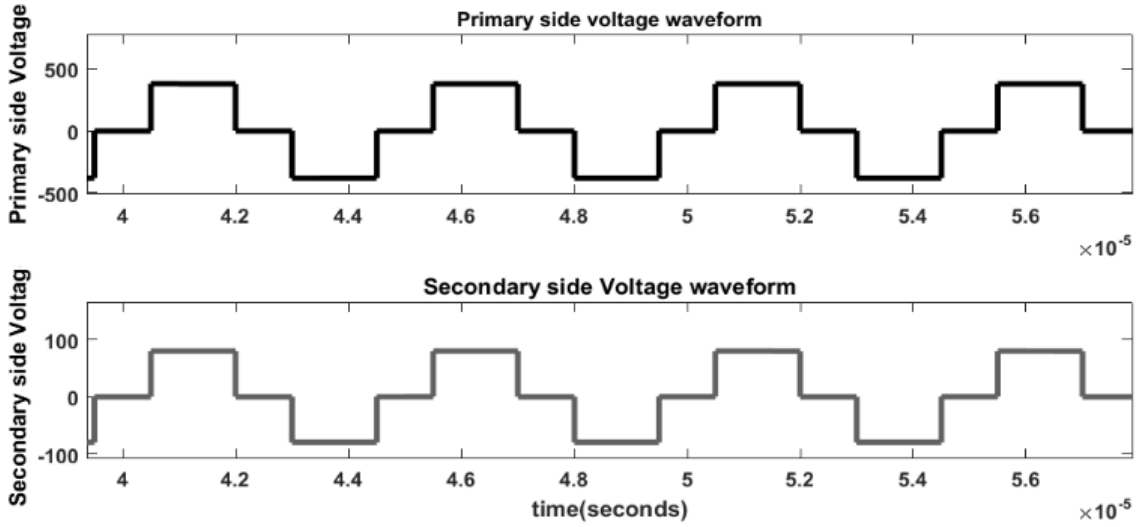

Fig.4.4 Primary and secondary side voltage waveform

In Figure 4.4, the primary and secondary side voltage waveform has been shown. The PI controller feedback loop controls the switches in order to maintain CC mode and the phase shift between the diagonal switches has been maintained which helps in attaining the desired voltage waveform at the primary and secondary sides. On both sides, the transformer has zero voltage due to the two upper switches or two lower switches.

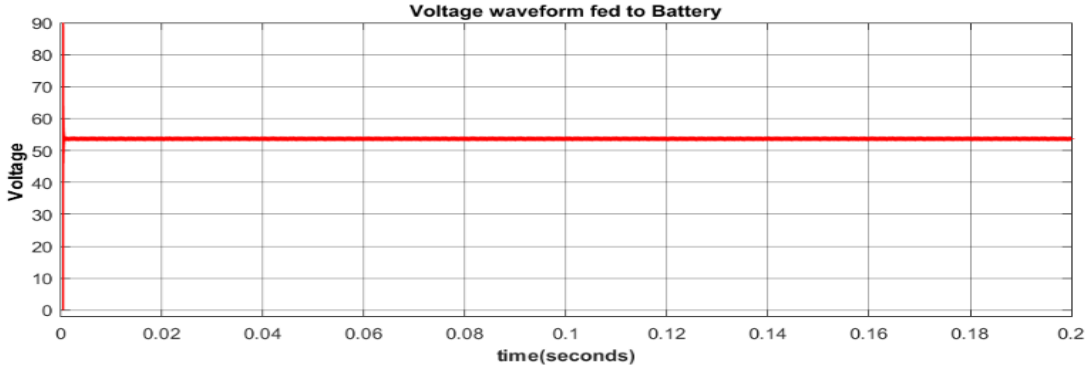

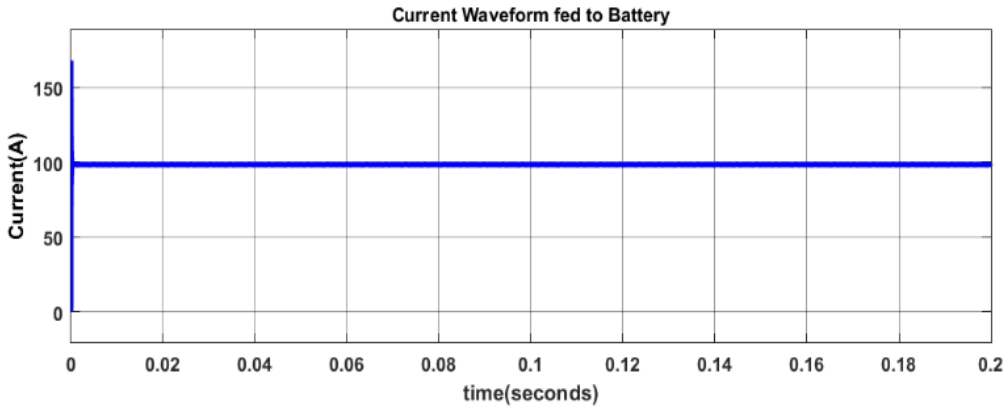

Fig.4.5 Output Voltage and current waveform fed to Battery

In Figure 4.5, the output voltage and current waveform is shown which comes after synchronous rectification through the secondary side of the high-frequency transformer. The output voltage is 55 V at the output of the converter and it is fed to the battery. The lithium-ion battery charges with a charging current of 100 A at initial SOC of 40 %.

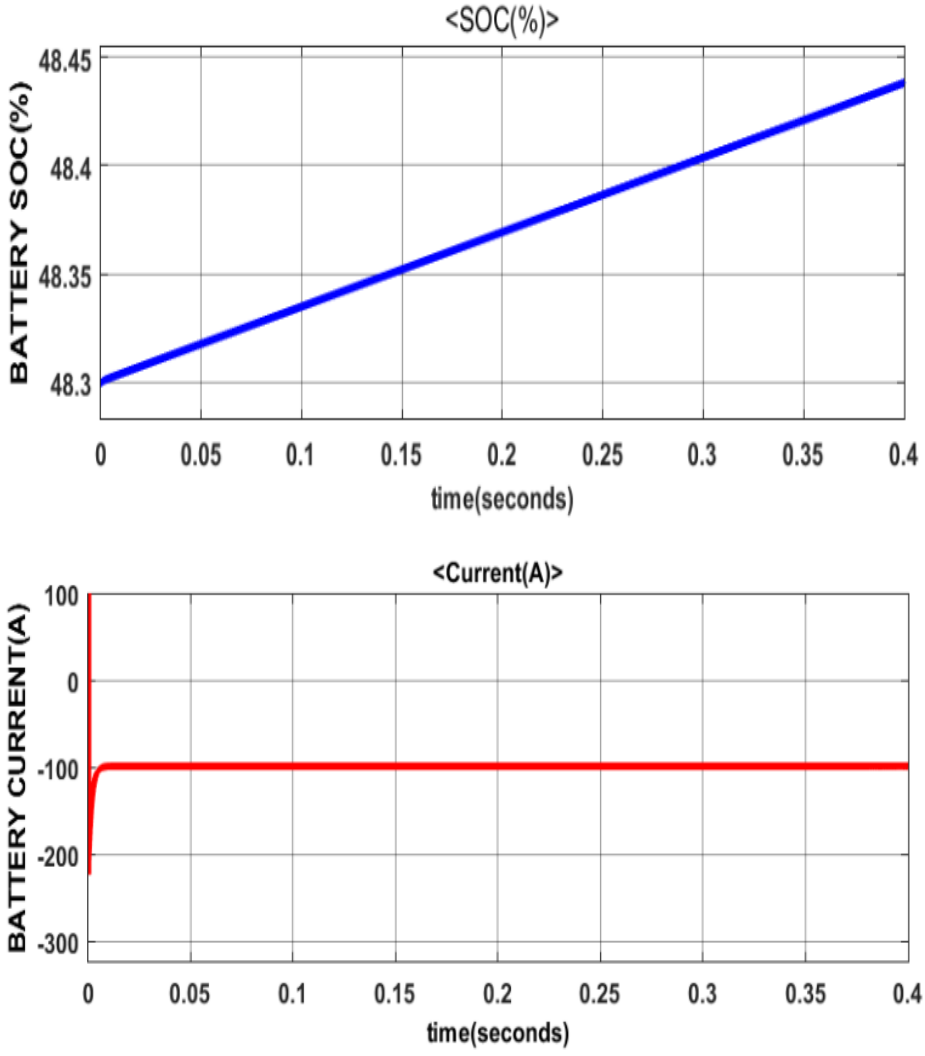

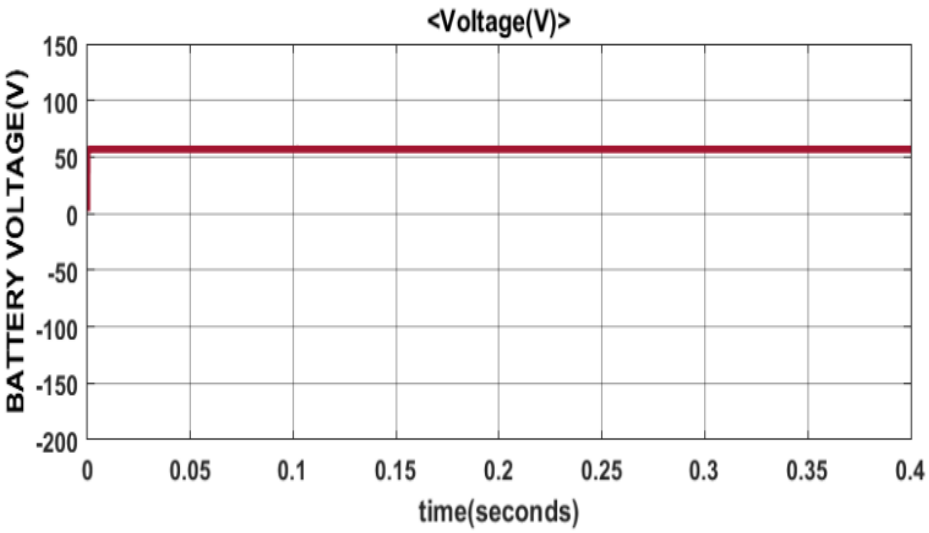

Fig.4.6 SOC, Current, Voltage waveform from the Battery

In Figure 4.6 the charging current remains almost constant up to 60% to 70 % of SOC and then the charging current starts decreasing gradually and at 99% SOC, the charging current becomes almost zero.

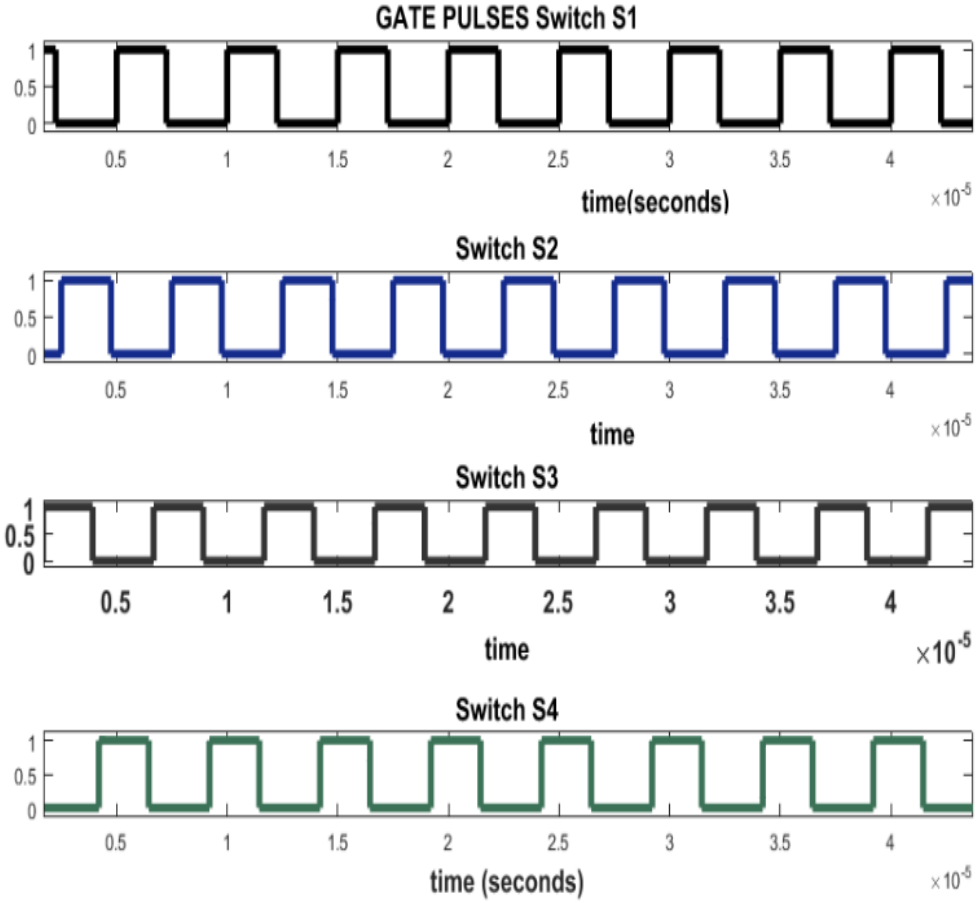

Fig.4.7 Switching Pulses

Figure 4.7 shows the switching pulses for switches S_1, S_2, S_3, S_4. The closed loop PI control has controlled the switching pulses in order to maintain the desired output.

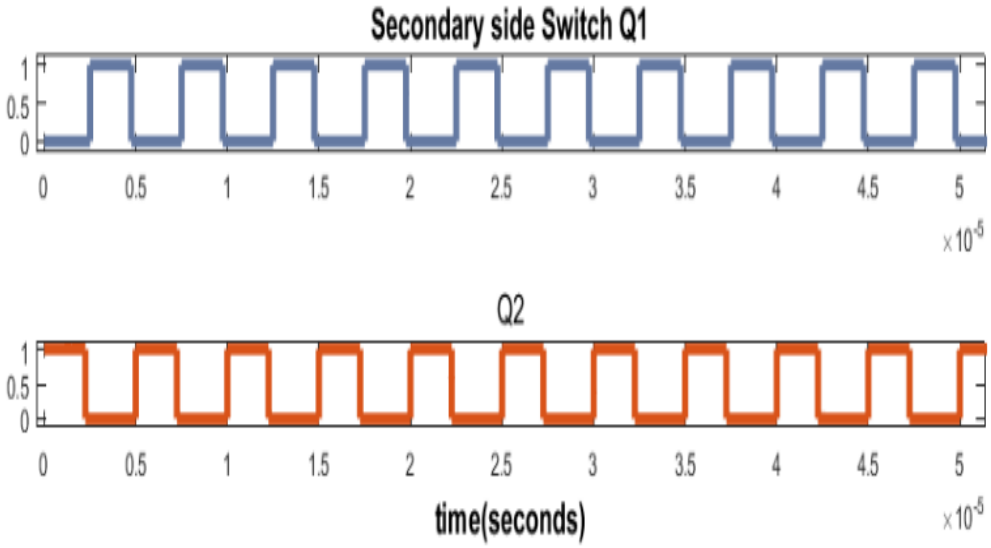

Fig.4.8 Switching Pulse at Q1, Q2

Figure 4.8 shows the switching pulse waveform at the secondary side switches Q_1 and Q_2.

4.4 CONCLUSION

In the proposed model, the charging of a 48V lithium-ion Battery through PSFB dc-dc converter closed-loop control has been studied in a SIMULINK environment. One PI controller has been used to maintain CC mode charging. The PI controller has a significant role in avoiding overshoots and undershoots for the charging current and has a faster response. SOC, current, and voltage waveforms of the battery have been presented for the charging state. PSFB dc-dc converter with synchronous rectification can be used for EV battery charging as it has high efficiency and enhances ZVS over a wide load range. The CC mode also helps in maintaining the life of the battery. The future scope of this paper can be extended to CC-CV charging and other Artificial Intelligence (AI) based control methods can be implemented.

CHAPTER 5
CONCLUSIONS AND FUTURE SCOPE

5.1 CONCLUSIONS

A 200 kHz switching frequency ZVS PSFB dc-dc converter and PSFB with Synchronous Rectifier have been Modeled in the Simulink environment. PSFB is preferred in EV battery charging applications and it supports ZVS over a wide load range. It is more efficient to run PSFB with Synchronous Rectification for higher efficiency. The model was analyzed under various loading conditions. The closed-loop model is analyzed and the charging of a 48V Lithium-ion Battery has been studied in a Simulink environment. Through the completion of this thesis study, several significant learning points have been identified, like, when high-power and high-frequency operation is involved, parasitics of the power electronic components play a crucial role and another is that High voltage track isolation requires significant effort.

The phase-shifted full bridge converter is a power electronic converter widely used in various applications such as renewable energy systems, electric vehicle chargers, and high-power server power supplies. It offers several advantages, including high efficiency, robustness, and the ability to work in ZVS over a wide load range. It is a reliable and efficient solution for power conversion. Its ability to control the phase shift between the switching signals allows for soft switching, reducing switching losses and improving overall efficiency. Additionally, its modular structure and scalability make it suitable for a wide range of power levels.

5.2 FUTURE SCOPE

Some of the recommendations for future scope are:

1. Future research can focus on optimizing the converter’s design and utilizing advanced semiconductor devices to achieve higher power density without compromising efficiency and reliability.
2. Wide bandgap semiconductor devices, such as silicon carbide (SiC) and gallium nitride (GaN), offer superior switching characteristics and higher operating temperatures compared to traditional silicon-based devices.
3. Developing advanced control algorithms and techniques can enhance the converter's dynamic response, transient performance, and fault tolerance. This

includes adaptive control strategies, predictive control, and advanced modulation techniques to further optimize the converter's efficiency and response to varying load conditions.

4. The integration of energy storage systems, such as batteries or supercapacitors, with the phase-shifted full bridge converter can enable energy management and improve grid interaction. This combination can lead to enhanced grid stability, peak shaving, and the ability to handle intermittent energy sources more effectively.
5. The phase-shifted full bridge converter can find new applications in emerging fields such as renewable energy integration, smart grids, and electric vehicle infrastructure. As these sectors continue to grow, the converter's ability to efficiently handle high power levels and provide reliable power conversion will be of great significance.

Continued research and development in areas such as power density, semiconductor integration, advanced control techniques, energy storage integration, and emerging applications will further enhance its performance and broaden its scope for future applications.

REFERENCES

[1] B. Maclnnis and J. A. Krosnick. (Oct. 2020). Climate insights 2020: Electric vehicles. Resources for the Future (RFF). [Online]. Available: https://www.rff.org/publications/reports/climateinsights2020- electric-vehicles.

[2] United States Environmental Protection Agency. (Apr. 2021). Inventory of U.S. Greenhouse Gas Emissions and Sinks. [Online]. Available: https://www.epa.gov/ghgemissions/inventory-us-greenhouse-gasemissions-and-sinks.

[3] International Energy Agency. (Apr. 2021). Global EV Outlook. [Online]. Available: https://iea.blob.core.windows.net/assets/ed5f4484-f556-4110- 8c5c-4ede8bcba637/GlobalEVOutlook2021.pdf

[4] S. Shankar, S. Lekshmi and M. R. Anaghakrishnan, "A novel AC-AC converter using bridgeless flyback rectifier and flyback CCM inverter", In *2016 Biennial International*

[5] *Conference on Power and Energy Systems: Towards Sustainable Energy,* pp. 1-6, 2016.

[6] Monem, M.A., Trad, K., Omar, N., Hegazy, O., Mantels, B., Mulder, G., Van den Bossche, P. and Van Mierlo, J, "Lithium-ion batteries: Evaluation study of different charging methodologies based on aging process." Applied Energy, vol. 152, pp. 143-155, 2015.

[7] M. Grenier, M. H. Aghdam, and T. Thiringer, "Design of on-board charger for plug-in hybrid electric vehicle," in Proc. Power Electronics, Machine and Drives Conference, pp. 1-6, 2010.

[8] S. Chothe, R. T. Ugale and A. Gambhir, "Design and modeling of Phase Shifted Full Bridge DC-DC Converter with ZVS," 2021 *National Power Electronics Conference (NPEC),* Bhubaneswar, India, 2021, pp. 01-06, doi: 10.1109/NPEC52100.2021.9672529.

[9] Texas Instruments, Phase-Shifted Full-Bridge, Zero-Voltage Transition Design Considerations - *Application report*", 2019.

[10] J. K. Sahoo and A. T. Mathew, "Design of a ZCS full — Bridge DC — DC converter for PV based electric vehicle fast charging station," *2017 IEEE Region 10 Symposium (TENSYMP),* 2017, pp. 1-5, doi: 10.1109/TENCONSpring.2017.8070079.

[11] F. Musavi, M. Craciun, D. S. Gautam, W. Eberle, and W. A. Dunford, "An LLC resonant DC–DC converter for wide output voltage range battery charging applications," IEEE Trans. Power Electron., Vol. 28, No. 12, pp. 5437-5445, Mar. 2013.

[12] E. Pool-Mazun, J. J. Sandoval, P. Enjeti and I. J. Pitel, "A Direct SwitchMode Three-Phase AC to DC Rectifier with High-Frequency Isolation for Fast EV Battery Chargers," 2019 *IEEE Applied Power Electronics Conference and Exposition (APEC),* 2019, pp. 573-580, doi: 10.1109/APEC.2019.8722237.

[13] Chakraborty, Sajib et al. "DC-DC Converter Topologies for Electric Vehicles, Plug-in Hybrid Electric Vehicles and Fast Charging Stations: State of the Art and Future [1]Trends." *Energies* (2019).

[14] Forecasting report of IHS automotive Q4/2018, 2018.

[15] B. Maclnnis and J. A. Krosnick. (Oct. 2020). Climate insights 2020: Electric vehicles. Resources for the Future (RFF). [Online]. Available: https://www.rff.org/publications/reports/climateinsights2020- electric-vehicles.

[16] e-amrit.niti.gov.in/benefits-of-electric-vehicles

[17] S. Harika, R. Seyezhai, and A. Jawahar, "*Investigation of DC Fast Charging Topologies for Electric Vehicle Charging Station (EVCS*)," IEEE Reg. 10 Annu. Int. Conf. Proceedings/TENCON, vol. 2019-Octob, pp. 1148–1153, 2019, doi: 10.1109/TENCON.2019.8929621.

[18] Expo. - APEC, pp. 1127– 1133, 2012 [5] S. Chauhan and N. R. Tummuru, "*High frequency AC Link Based Isolated Dual Active Bridge DC-DC Converter Control, Features and Its Functionalities*," in Proc. Of IEEE International Conference on Power Electronics, Smart Grid and Renewable Energy (PESGRE2020), Cochin, India, 2020, pp. 1-6.

[19] [M. Safayatullah, M. T. Elrais, S. Ghosh, R. Rezaii and I. Batarseh, "A Comprehensive Review of Power Converter Topologies and Control Methods for Electric Vehicle Fast Charging Applications," in IEEE Access, vol. 10, pp. 40753-40793, 2022, doi: 10.1109/ACCESS.2022.3166935.

[20] Chakraborty, Sajib et al. "DC-DC Converter Topologies for Electric Vehicles, Plug-in Hybrid Electric Vehicles and Fast Charging Stations: State of the Art and Future [Trends." Energies (2019).

[21] S. Chothe, R. T. Ugale and A. Gambhir, "Design and modeling of Phase Shifted Full Bridge DC-DC Converter with ZVS," 2021 National Power Electronics Conference (NPEC), Bhubaneswar, India, 2021, pp. 01-06, doi: 10.1109/NPEC52100.2021.9672529.

[22] Texas Instruments; Phase-Shifted Full-Bridge Controller with Synchronous Rectification (2012).

[23] Ş. Küçük and E. Akboy, "A Basic Phase Shift Full Bridge DC-DC Converter Design And Simulation," 2022 57th International Universities Power Engineering Conference (UPEC), Istanbul, Turkey, 2022, pp. 1- 7, doi: 10.1109/UPEC55022.2022.9917909.

[24] Murat Yilmaz, and Philip T. Krein, "Review of Battery Charger Topologies, Charging Power Levels, and Infrastructure for Plug-In Electric and Hybrid Vehicles", IEEE transactions on power elec., vol. 28, no. 5.

[25] A. Ayob, W. M. F. W. Mahmood, A. Mohamed , M. Z. C Wanik, "Review on Electric Vehicle, Battery Charger, Charging Station and Standards", Research Journal of Applied Sciences, Engineering and Technology, ISSN: 2040-7459; eISSN: 2040-7467.

[26] E. L. Carvalho, E. G. Carati, J. P. da Costa, C. M. de Oliveira Stein and R. Cardoso, "Analysis, design and implementation of an isolated full-bridge converter for battery charging," Brazilian Power Electronics Conference (COBEP), pp. 1-6, Nov 2017.

[27] J. C. Mukherjee and A. Gupta, "A Review of Charge Scheduling of Electric Vehicles in Smart Grid," *IEEE Systems Journal*, vol. 9, pp. 1541-1553, 2015.

[28] N. Mohan and T. M. Undeland, Power electronics: converters, applications, and design: John Wiley & Sons, 2007

[29] Watanabe, T. and Kurokawa, F. (2015). Efficiency comparison between phase shift and LLC converters as power supply for information and communication equipments. 2015 IEEE International Telecommunications Energy Conference (INTELEC).

[30] J. Sabate, V. Vlatkovic, R. Ridley, F. Lee, and B. Cho, "Design considerations for high-voltage high-power full-bridge zero-voltageswitched PWM converter," in Proc. IEEE APE

[31] Tsukiyama, D., Fukuda, Y., Miyake, S., Mekhilef, S., Kwon, S. and Nakaoka, M. (2011). A new 98% soft-switching full-bridge DC-DC converter based on secondary-side LC resonant principle for PV generation systems. 2011 IEEE Ninth International Conference on Power Electronics and Drive Systems.

[32] M. K. Kazimierczuk, Pulse-width modulated DC-DC power converters: John Wiley & Sons, 2008.

[33] Z. Emami, M. Nikpendar, N. Shafiei and S. Motahari, ”Leading and lagging legs power loss analysis in ZVS Phase-Shift Full Bridge converter”, 2011 2nd Power Electronics, Drive Systems and Technologies Conference, 2011.

[34] Yang, B., Duarte, J., Li, W., Yin, K., He, X. and Deng, Y. (2010). Phase-shifted full bridge converter featuring ZVS over the full load range. IECON 2010 - 36th Annual Conference on IEEE Industrial Electronics Society.

[35] Di Capua, G., Shirsavar, S., Hallworth, M. and Femia, N. (2015). An Enhanced Model for Small-Signal Analysis of the Phase-Shifted Full-Bridge Converter. IEEE Transactions on Power Electronics, 30(3), pp.1567-1576.

[36]] U. Badstuebner, J. Biela, and J. W. Kolar, “Design of an 99%-efficient, 5kW, phase-shift PWM DC-DC converter for telecom applications,” in Proc. Applied Power Electronics Conference and Exposition (APEC), pp. 626-634, 2010.

[37] Shi, K., Zhang, D., Zhou, Z., Zhang, M. and Gu, Y. (2016). A Novel Phase-Shift Dual Full-Bridge Converter With Full Soft-Switching Range and Wide Conversion Range. IEEE Transactions on Power Electronics, 31(11), pp.7747-7760.

[38] X. Ruan, Soft-switching PWM full-Bridge converters: topologies, control, and design. Wiley, 2014.

[39] Z. Ouyang, J. Zhang and W. G. Hurley, “Calculation of Leakage Inductance for High-Frequency Transformers,” IEEE Trans. on Power Electron., vol. 30, no. 10, pp. 5769-5775, Oct. 2015.

[40] C. Zhong, J. Biao, J. Feng, and S. Lei, “Analysis and design considerations of an improved ZVS full-bridge DC-DC converter,” in Proc. IEEE Applied Power Electronics Conference and Exposition (APEC), 2010, pp. 1471-1476.

[41] W. Xinke, Z. Junming, X. Xiaogao, and Q. Zhaoming, “Analysis and optimal design considerations for an improved full bridge ZVS DC-DC converter with high efficiency,” IEEE Trans. Power Electron., vol. 21, no. 5, pp. 1225-1234, Sep. 2006.

[42]] Y. D. Kim, K. M. Cho, D. Y. Kim, and G. W. Moon, “Wide-range ZVS phase-shift full-bridge converter with reduced conduction loss caused by circulating current,” IEEE Trans. Power Electron., vol. 28, no. 7, pp. 3308-3316, Jul. 2013.

[43] G. Di Capua, S. A. Shirsavar, M. A. Hallworth, and N. Femia, "An enhanced model for small-signal analysis of the phase-shifted fullbridge converter," Power Electronics, IEEE Transactions on, vol. 30, pp. 1567-1576, 2015.

[44] K. V. R. Kishore, B. F. Wang, K. N. Kumar and P. L. So, “A new ZVS full-bridge DC-DC converter for battery charging with reduced losses over full-load range,” in Proc. IEEE India International Conference (INDICON), New Delhi, 2015, pp. 1-6.

[45] M. Yilmaz and P. T. Krein, “Review of battery charger topologies, charging power levels, and infrastructure for plug-in electric and hybrid vehicles,” IEEE Trans. Power Electron., vol. 28, no. 5, pp. 2151-2169, May 2013.

[46] B. Whitaker, A. Barkley, Z. Cole, B. Passmore, D. Martin, T. R. McNutt, A. B. Lostetter, J. S. Lee, and K. Shiozaki, “A high-density, high-efficiency, isolated on-board vehicle battery charger utilizing silicon carbide power devices,” IEEE Trans. Power Electron., vol. 29, no. 5, pp. 2606-2617, May 2014.

[47] Y. Bingjian, J. L. Duarte, L. Wuhua, Y. Kai, H. Xiangning, and D. Yan, “Phase-shifted full bridge converter featuring ZVS over the full load range,” in Proc. Annual IEEE Industrial Electronics Society Conference (IECON), 2010, pp. 644-649.

[48] A. Y. Saber and G. K. Venayagamoorthy, “Plug-in vehicles and renewable energy sources for cost and emission reductions,” IEEE Trans. Ind. Electron., vol. 58, no. 4, pp. 1229-1238, Apr. 2011.

[49] S. Cetin and A. Astepe, “A phase shifted full bridge converter design for electrical vehicle battery charge applications based on wide output voltage range,” in Proc. of 21st Applied Electronics, pp. 51-56, 2016.

[50] J. W. Kim, D. Y. Kim, C. E. Kim, and G. W. Moon, “Simple switching control technique for improving light load efficiency in a phase-shifted full-bridge converter with a server power system,” IEEE Trans. Power Electron., Vol. 29, No. 4, pp. 1562-1566, Apr. 2014.

[51] Fu Yingjie, et al." Multi-redundancy uninterruptible on-board high voltage power supply system." Movable Power Station & Vehicle 2(2017).

[52] D. Aggeler, F. Canales, H. Zelaya - De La Parra, A. Coccia, N. Butcher, and O. Apeldoorn, “Ultra-Fast DC-Charge Infrastructures for EVMobility and Future Smart Grids,” Innovative Smart Grid Technologies Conference Europe (ISGT Europe), 2010 IEEE PES

[53] G. Di Capua, S. A. Shirsavar, M. A. Hallworth, and N. Femia, "An enhanced model for small-signal analysis of the phase-shifted fullbridge converter," Power Electronics, IEEE Transactions on, vol. 30, pp. 1567-1576, 2015.

LIST OF PUBLICATIONS

[1] Awanish Akash, Mini Sreejeth "High-Frequency DC-DC Isolated Converter with Rectification and Synchronous Rectification", *IEEE 4th International Conference of Emerging Technologies 2023*, Belgaum, Karnataka, India(26-28 May 2022) **(Presented)**

[2] Awanish Akash, Mini Sreejeth "Isolated DC-DC Converter with Synchronous Rectification for Electric Vehicle Battery Charging", *IEEE 3rd International Conference for Intelligent Technologies, 2023, Hubballi, Karnataka, India* **(Accepted)**

Certificate

Jain College of Engineering
Belagavi, India

IEEE BANGALORE SECTION

4th International Conference of Emerging Technology
(INCET 2023)

26th – 28th May 2023

Certificate

This is to certify that Dr./Prof./Mr./Ms. ***Awanish Akash*** *has presented paper entitled* ***High Frequency DC DC Isolated Converter with Rectification and Synchronous Rectification*** *in 4th International Conference of Emerging Technology (INCET 2023) during 26th to 28th May 2023.*

Dr. Krupa Rasane
Convener - INCET 2023

Dr. J. Shivakumar
General Chair - INCET 2023